Aus dem Deutschen Herzzentrum Berlin

Dissertation

Reliability of Echocardiographic Myocardial Deformation Analysis by Speckle Tracking Imaging for Prediction of Patients with Cardiac Allograft Vasculopathy after Heart Transplantation

Zur Erlangung des akademischen Grades
Doktor medicinae (Dr. med.)

vorgelegt der Medizinischen Fakultät
Charité – Universitätsmedizin Berlin

von

Chol Ho, Pang
aus S.Pyongan, DVR Korea

Gutachter/in: 1. Priv.-Doz. Dr. med. M. Dandel
2. Prof. Dr. med. J. Ennker
3. Prof. Dr. med. B. Stiller

Datum der Promotion: 03.06.2012

Contents

Abbreviations

2CH	apical two-chamber view
4CH	apical four-chamber view
2D	two-dimensional
A	late diastolic filling velocity
APLAX	apical long-axis
AR	acute rejection
AUC	area under the curve
BMI	body mass index
BSA	body surface area
CAV	cardiac allograft vasculopathy
CFR	coronary flow reserve
CI	cardiac index, confidence interval
CRT	cardiac resynchronization therapy
CS_t	total coronary calcium score
DBP	diastolic blood pressure
DSE	dobutamine stress echocardiography
DT	deceleration time
E	early diastolic filling velocity
EBCT	electron beam computed tomography
EF	ejection fraction
FS	fractional shortening
GS	global peak systolic strain
GSr	global peak systolic strain rate
GSrA	global late diastolic strain rate
GSrE	global early diastolic strain rate
GSrE/TpSrE	acceleration of early diastolic deformation
GSr/TpSr	acceleration of systolic deformation
HTx	heart transplantation
$Index_{asynch.}$	intraventricular asynchrony index
IVRT	isovolumic relaxation time
IVS	interventricular septum
LA	left atrial
LV	left ventricle; left ventricular
LVEDP,	LV end-diastolic pressure
$LVID_{d,s}$	LV internal dimension in diastole, systole
MRI	magnetic resonance imaging
NPV	negative predictive value
PAP	pulmonary artery pressure
PCWP	pulmonary capillary wedge pressure
PET	positron emission tomography
PHT	pressure half time
PPV	positive predictive value
PW	pulsed wave, posterior wall
RA	right atrial pressure
ROC	receiver operating characteristics
RV	right ventricle; right ventricular
RWT	relative wall thickness
SAX	parasternal short-axis views at the level of mitral valve
$S_{disp.}$	peak systolic strain dispersion

$S_{disp.}(r)$	peak systolic strain relative dispersion
SBP	systolic blood pressure
SD_{TpS}	one standard deviation of the time to peak systolic strain
Sr	strain rate
STE	speckle tracking echocardiography
TDI	tissue Doppler imaging
TpSr	time to peak systolic strain rate
TpSrC	time to peak circumferential systolic strain rate
TpSrE	time to peak diastolic early strain rate
TpSrL	time to peak longitudinal systolic strain rate
$TpS_{disp.}$	dispersion of time to peak systolic strain
TpSr/TpSrE	ratio of time to peak systolic and diastolic strain rate
US	ultrasound
WMA	wall motion abnormality(ies)

1. Introduction

The number of heart transplants being performed worldwide exceeds 5,000 per year and the 10 year survival probability after transplant reaches 50%.[1]

The major cardiac long-term complication that occurs in heart transplant recipients is the development of transplant or cardiac allograft vasculopathy, which is an entity distinct from native coronary disease of the nontransplanted heart. Cardiac allograft vasculopathy (CAV), characterized by intimal proliferation, develops early after transplant, and is progressive.[2] CAV after transplant develops with an incidence of 8% at 1 year, 20% at 3 years, 30% at 5 years, and more than 50% at 10 years and is the third cause of death after heart transplant, being responsible for 10-15% of deaths.[1]

The diagnosis of CAV is difficult because of denervation as well as the concentric and diffuse nature of the disease. The lack of early clinical symptoms due to myocardial ischemia such as classical angina makes patients with CAV present late with silent myocardial infarction, congestive heart failure, or ventricular arrhythmia leading to syncope or sudden death.[3,4]

Early diagnosis of CAV is important because the prevention of impending catastrophic events is feasible in some patients through revascularization either percutaneously with balloon angioplasty with or without stent implantation, or by means of bypass surgery.

Coronary angiography in combination with intravascular ultrasound (IVUS) is currently the gold standard for CAV diagnosis. The annually performance of coronary angiography for CAV surveillance, however, poses the risks associated with the invasive method and because of the accelerated nature of the vasculopathy may be even insufficient for early CAV diagnosis.

Efforts for the optimal timing of coronary angiography using non-invasive methods are gaining acceptance in clinical practice.[5,57]

2. Background

2.1. Cardiac Allograft Vasculopathy Surveillance

2.1.1. Invasive Methods

2.1.1.1. Coronary Angiography

Coronary angiography remains the standard of CAV diagnosis [6].

The morphologic findings in coronary angiograms of transplant coronary disease differ greatly from angiographic features in typical nontransplant patients with coronary artery disease (CAD), which is usually a focal, eccentric stenosis in epicardial coronary vessels. The Stanford classification system has been developed to describe lesion morphologies commonly seen at angiography in heart transplant recipients with CAV and is being used in the angiographic assessment for CAV.[7] With this system Gao et al initially described the anatomic abnormalities with the classification into type A, B1, B2, and C lesions. Type A, similar to CAD in nontransplant patients, was discrete or tubular stenosis in the proximal, middle, or distal segment branches; type B1 was a proximal vessel maintaining normal diameter with abrupt distal concentric narrowing and obliteration; type B2 was a gradual transition from normal proximal vessel with smooth concentric tapering, the distal vessel having some residual lumen; and type C was narrowed irregular distal branches with loss of small branches. Most of the lesions of types B1, B2 and C appeared in the secondary vessels and tertiary vessels in patients with CAV, whereas no type B1, B2 or C lesions were seen in non-transplant CAD and all of the non-transplant angiographic lesions consisted of type A. In transplant patients, total occlusion appeared more commonly distally (49%) and without absence of collateral circulation as compared with non-transplant angiographic lesions ($p < 0.002$).

Coronary angiography has been shown to be acceptably specific but insufficiently sensitive in the diagnosis of CAV, except for significant focal stenoses. [8-11] In a prospective comparative study of coronary angiography and IVUS, the specificity of coronary angiographic prediction (89%) was satisfactory but its sensitivity (43%) was low.[10] Johnson et al[12] showed that 73% of the angiographically normal segments in patients who had graft failure within 2 months of coronary angiography showed mild to moderate fibrous intimal thickening by light microscopy but angiographic comparisons of the degree of luminal narrowing showed good correlation for focal stenoses. The insensitivity of coronary angiography in CAV diagnosis has been also demonstrated by comparison with IVUS.[13]

The very nature of angiography limits the ability to measure anything that is not represented well by luminal imaging, stressing that angiograms should be interpreted serially, as new and concentric lesions may be missed on one-time angiograms.[34] Serial quantitative coronary angiography has been shown to be important in the assessment of the progression of CAD.[8,9,14,15]
By using quantitative angiography with cine-videodensitometry in 18 "angiographically normal" heart transplant recipients, Mills et al[15] demonstrated significant loss of lumen diameter between years 1 and 3, emphasizing that angiograms should be interpreted serially as new and concentric lesions may be overlooked on one-time angiograms.
Coronary angiography has been showed to be useful in predicting cardiac events from CAV. Uretsky et al[4] showed that the relative risk (odds ratio) of any cardiac event, including myocardial infarction, heart failure, and sudden death, was 3.44 ($p < 0.05$) in patients with angiographic evidence of obstructive disease compared with those without evidence of disease, or risk of cardiac death 4.6($p < 0.05$). Keogh et al[16] showed that survival for single-vessel disease (40% or greater) was 64% at 1 year, 36% at 2 years, and 22% at 5 years and for triple-vessel disease it was significantly worse (13% at 2 years; $p=0.01$). The cardiac event free survival rate in the patients with negative angiography results was 96% at 4 years of follow-up.[17]

In most heart transplant centers, routine coronary angiography is performed shortly after transplantation to determine baseline coronary characteristics and is subsequently done annually for CAV surveillance.[18] However, with routine coronary angiography there are risks of complications, especially renal failure, because of the exposure of patients on nephrotoxic immunosuppressive medication to radiocontrast.[19]

2.1.1.2. Intravascular Ultrasound

Intravascular ultrasound (IVUS) is the most sensitive tool for the diagnosis of CAV.
St. Goar et al[13] compared firstly in vivo IVUS with angiograhpy in cardiac transplant recipients and showed the intimal thickening was abnormal 1 year or more after transplantation in a group of patients with normal angiograms (angiographically silent intimal thickening) and was not significantly different in those patients with abnormal angiograms.
Studies demonstrated that IVUS is superior to coronary angiography in detecting early intimal thickening of the coronary vessels.[20,21] In a study by Pflugfelder et al[20], there were angiographic abnormalities in only 15% of the vessel segments examined but IVUS identified 34%

pathological cross-sectional areas. Kerber et al[21] demonstrated that, early after transplantation, angiography reveals only gross coronary abnormalities whereas IVUS showed already intimal thickening of a moderate degree in 42% of the examined coronary vessel segments. IVUS showed CAV in 75% of patients at 1 year after heart transplantation, whereas angiography detected CAV in only 10% -20%.[22,23]

The Stanford classification [13] for the assessment of CAV severity was developed according to intimal thickness and degree of vessel circumference involved: class I (minimal), an intimal layer less than 0.3mm thick measurable in less than 180^0 of the vessel circumference; class II (mild), an intimal layer less than 0.3mm but measurable in more than 180^0 of the vessel circumference; class III (moderate), an intimal layer 0.3-0.5mm thick or an intimal layer more than 0.5mm thick involving less than 180^0 of the vessel circumference; and class IV (severe), more than 0.5mm intimal thickening involving more than 180^0 of the vessel circumference or an intimal layer greater than 1.0mm in any one area of the vessel circumference.

The presence of moderate to severe intimal thickening as shown by IVUS has been demonstrated to be predictive of the future development of angiographically apparent CAV. Rapidly progressive CAV, defined as an increase of ≧0.5mm in maximal intimal thickness within the first year after HTx, is associated with a significantly increased risk of all-cause death, myocardial infarction, and the subsequent development of angiographically severe CAV.[24,25]

Bocksch et al[26] showed that serial IVUS is highly reproducible with a correlation coefficient for thickness of plaques of 0.96 for interobserver agreement.

The safety of IVUS has been well documented.[27,28] The reported complications include focal coronary spasm, vessel dissection, guidewire entrapment and acute occlusion, resulting in myocardial infarction, which occurs in < 1.1% of procedures.[28] Repeated IVUS after HTx has been shown not to be associated with acceleration of CAV.[27,29]

Although IVUS is a sensitive and safe method for the prediction and surveillance of CAV, several problems of IVUS limit its widespread use.[3] IVUS can only be used to analyze the proximal large vessels, not secondary or tertiary vessels, where CAV is first evident. The cost and invasiveness are also major limiting factors. The question needs to be answered, whether IVUS is superior to angiography for making therapeutic decisions rather than diagnostic strategies.

2.1.2. Non-invasive Methods

In general, noninvasive methods have not been sensitive or specific enough to be reliable to screen for CAV. However, repeated invasive methods pose increased risks for the patients and may be insufficient for early diagnosis because of the accelerative nature of the disease. Therefore, optimal timing of invasive methods by non-invasive methods, which are easily available without risks, may be efficient in the clinical practice after HTx and such efforts are gaining clinical acceptance.

2.1.2.1. Electrocardiography

There are few studies regarding the role of exercise electrocardigraphy in the diagnosis of CAV. Mairesse et al[30] showed, in a group of patients with no hemodynamically significant (>50% diameter) coronary stenosis, that the exercise electrocardiogram was interpretable in only 59% of the patients. In a study by Smart et al[31], the sensitivity and specificity of supine exercise testing for CAV were 21% and 77%, respectively. For exercise treadmill testing, Ehrman et al[32] reported specificity of 90%.

In a follow-up study of 39 patients, Bacal et al[33] showed low sensitivity (15%) of ambulatory electrocardiography in the diagnosis of CAV.

There are some limiting factors that have an influence on the results of exercise electrocardiography. These include abnormal baseline electrocardiograms showing abnormal repolarization, lack of ischemia- induced angina and frequently inability to reach 85% of the maximal heart rate.[34]

2.1.2.2. Echocardiography

Echocardiography, which provides comprehensive information about cardiac structure and function, is a primary non-invasive method in the management after HTx. Echocardigraphic examinations can be easily performed at the bedside and serially repeated without any discomfort to patients.

2.1.2.2.1 .Conventional Echocardiography

Early after transplantation, left ventricular (LV) mass and end-diastolic volume (EDV) increase, and these changes may or may not persist for years, without being predictive of long-term results[35,36]. Wilhelmi et al[37] demonstrated left atrial (LA) and ventricular dimensions within

normal ranges (LA 37.3 ± 8.9 mm, LV enddiastolic dimension 45.6 ± 6.4 mm), and normal mean ejection fraction (EF) of 71 ± 11.7% and fractional shortening of 35.3 ± 10.3% in 65 patients more than 10 years after transplantation. The authors reported also left ventricular hypertrophy as a common finding, particularly late after transplantation, with calculated LV mass in males of 263.8 ± 111.4g and in females of 373.0 ± 181.1g. In contrast to systolic function, diastolic function is abnormal early after transplantation. A restrictive filling pattern, characterized by shorter isovolumetric relaxation time (IVRT; 65 ± 18 msec) and pressure half-time (PHT; 39 ± 8 msec), and higher early diastolic filling velocity (E; 0.77 ± 0.20 m/s), may persist to some degree chronically in some patients,[38] limiting the diagnostic value of echocardiographic diastolic parameters in heart transplant recipients with CAV.

Echocardiographic wall motion abnormalities (WMA) at rest have shown low sensitivity in the diagnosis of CAV.[31,39] Spes et al[40] showed that echocardiographic WMA at rest had a sensitivity of 57% (specificity 88%) in the diagnosis of CAV as defined by IVUS and angiography.

2.1.2.2.2. Stress Echocardiography and Myocardial Contrast Echocardiography

There has been much interest in the use of stress echocardiography, to determine its predictive and prognostic value in heart transplant recipients.

Exercise echocardiography has been shown to be insensitive in the diagnosis of CAV. In a group of 51 patients, Collings et al[41] showed that exercise echocardiography had a relative high specificity of 86% but a high false negative rate for the prediction of moderate coronary disease, defined as stenosis of 40% to 69%. Similarly, Cohn et al[42] showed a low sensitivity of 15% for the diagnosis of class III to IV intimal thickening and a specificity of 85%. The diffuse nature of CAV and abnormal heart rate response during exercise in transplant recipients seems to be associated with the insensitivity of exercise echocardiography.[34,42]

Ciliberto et al[43] showed that high-dose dipyridamole echocardiography had a sensitivity of 32% and a specificity of 100% for detecting CAV in 25 patients with CAV, compared with coronary angiography.

Dobutamine stress echocardiography (DSE) for assessment of wall motion has been the mostly frequently used method and has proven to be useful in the diagnosis and prognostic assessment of CAV. Günther et al[45] showed that DSE is feasible and safe in heart transplant recipients. Based on IVUS and coronary angiograms, Spes et al[46] divided 46 patients into two groups: Group 1 (n=18) had absent or only mild intimal hyperplasia (mean IVUS grade $\leq$3.0) and Group 2 (n=28) had moderate to severe intimal hyperplasia (mean grade >3 with or without

angiographic evidence of CAV). The WMA occurred significantly more frequently in group 2 than in group 1, both at rest and during maximal DSE, and the wall thickening decreased more significantly in group 2 than in group 1 during DSE in the septum and left ventricular posterior wall. This shows that DSE is a feasible noninvasive method for the detection of CAV after transplantation. Studies, which compared DSE with coronary angiography, showed a sensitivity of WBS to detect angiographic CAV of 95% and 86%, and a specificity of 55% and 91%, respectively.[44,47] In 144 heart transplant recipients, Spes et al[48], based on a combined angiographic and IVUS definition of CAV, showed a sensitivity of 76% and a specificity of 82%. The same group showed also that a quantitative measurement of systolic wall thickening during DSE improved the sensitivity of the 2D-DSE from 76% to 85%.

DSE has been also shown to be closely associated with prognostic information. Akosah et al[44,49] showed no cardiac events in patients with normal DSE in the 12- and 32 ±11 month follow-up study, respectively. In asymptomatic patients followed for 4 years after transplantation, Bacal et al[17] showed that 87.8% of the patients with normal DSE and only 29.6% of the patients with abnormal DSE were alive without cardiac events at 48 months of follow-up. Spes et al[50] prospectively evaluated heart transplant recipients with serial DSE and compared coronary angiography and IVUS in 109 heart transplant recipients followed for up to 5 years. Cardiac events occurred in only 1.9% of patients with normal DSE, compared with 6.3% of patients with normal resting studies, and serial DSE deterioration indicated a higher risk for subsequent cardiac events than no change (relative risk 7.26, p=0.0014). The prognostic value of DSE, however, is lower than that of coronary angiography.[17,50] Based on the results regarding the prognostic value of DSE, a new monitoring strategy, that invasive testing is reserved only for patients with greater risk of cardiac events[17] and postponed if DSE is normal beyond 1 year after HTx[50], has been proposed.

Stress echocardiography has the limitation that its interpretation is subjective and dependent greatly on experience.[51]

The measurement of a lower coronary flow rate with contrast-enhanced transthoracic echocardiography has showed promising results for detecting CAV[52-54] but may not be accessible to all patients. By combining contrast-enhanced echocardiography and adenosine-mediated hyperemia, Tona et al[55] compared coronary flow reserve with coronary angiography in 73 patients 8 years after HTx. A coronary flow reserve cut-off ≤ 2.7 had a sensitivity of 87% and specificity of 82% in the diagnosis of CAV. This group reported recently a sensitivity of 80%

and a specificity of 100% of a cut-off ≤2.9 for detecting of CAV, defined as maximal intimal thickness of ≧0.5mm in IVUS.[56]

2.1.2.2.3. Myocardial Velocity Imaging by pulsed Doppler

Myocardial velocity imaging is now an established clinical method for quantifying LV systolic and diastolic function.

In 363 heart transplant recipients, Dandel et al[57] demonstrated for the first time the reliability of LV wall motion assessment by pulsed wave tissue Doppler imaging (PW-TDI) in the prediction of CAV. A series of PW-TDI parameters, peak systolic wall motion velocity (Sm), systolic time (TSm, from onset of first heart sound to the peak of the systolic wave Sm) and systolic wall acceleration (Sm/TSm), had high positive and negative predictive values: positive and negative predictive value of 97.73% at Sm ≤10 cm/s and Sm ≥11cm/s, respectively. Based on the promising results for the diagnosis of CAV with PW-TDI[43-2] and electron beam computed tomography (EBCT)[58], a noninvasive surveillance strategy for early identification of heart transplant recipients with possible coronary stenoses has been developed (Figure 1).[59]

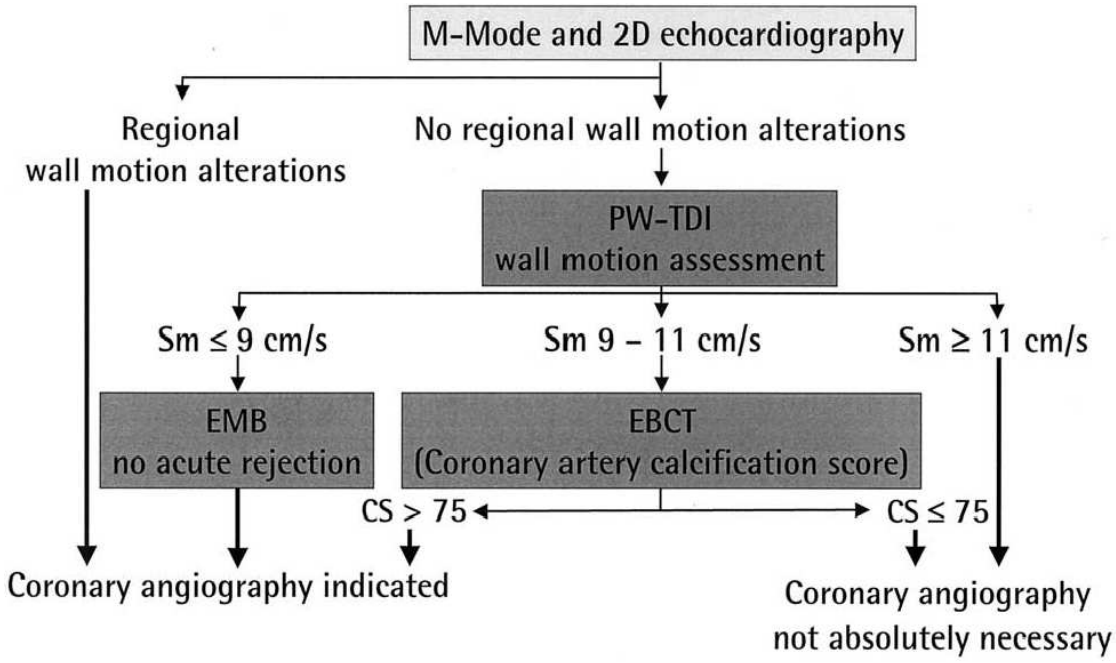

Figure 1. Diagnostic prediction for coronary stenoses in heart transplant recipients by combined EBCT and PW-TDI monitoring.

At the Deutsches Herzzentrum Berlin PW-TDI has been routinely used since 1998 and has become an important part of echocardiography for the monitoring of cardiac allograft function and for the timing of invasive testing.

PW-TDI, especially Sm, is relatively less image quality dependent for measurement and although it is angle dependent, when the highest velocity from at least 5 tracings is selected, it is highly reproducible.[57] There were no significant differences of the systolic PW-TDI parameters, obtained at the posterior wall, between patients with or without proximal stenoses of the great epicardial vessels, showing that although PW-TDI velocities are obtained only from one region at a time, they reflect the functional state of large myocardial areas in patients of CAV, which is characterized by its diffuse nature. The PW-TDI systolic parameters are, similar to LVEF, load dependent.

2.1.2.3. Other Methods

2.1.2.3.1. Single-Photon Emission Computed Tomography

Myocardial single-photon emission computed tomography (SPECT) has proven its value in detecting native coronary artery disease. Many studies assessed the diagnostic value of myocardial scintigraphy in the prediction of CAV, showing conflicting data regarding the sensitivity and specificity.

Exercise ^{201}Tl myocardial perfusion imaging has shown sensitivity varying from 67% to 78% and specificity ranging from 33% to 100% in prediction of CAV.[60,61,62] Ciliberto et al[60] studied 50 heart transplant recipients. Exercise thallium scintigraphy was negative in all of the 35 patients with normal coronary arteries (specificity, 100%), and abnormal in 10 of 15 patients with CAV (sensitivity, 67%).

Pharmacologic stress using dipyridamole showed sensitivities of 21% to 58% and specificities of 64% to 88%.[31,63] Carlsen et al[64] compared dipyridamole-99m-Tc-sestamibi myocardial scintigraphy with CAG in 67 transplant recipients during a follow-up period of 5.6 years and showed a high negative predictive value of SPECT (98%) in screening for significant CAV, concluding that annual myocardial stress perfusion scintigraphy seems well suited as a screening method for detecting significant CAV.

Wu et al[65] showed that dobutamine ^{201}Tl SPECT is highly sensitive and negatively predictive for prediction of angiographic CAV (sensitivity, specificity, positive predictive value and negative predictive value, were 89%, 71%, 42% and 96%, respectively). Elhendy et al[66] studied 50 patients, using tetrofosmin as tracer. Dobutamine 99m technetium tetrofosmin SPECT was

positive in 27 of 30 patients with angiographic CAV (sensitivity, 90%) and negative in 9 of 20 patients without significant CAV (specificity, 55%).

Although several studies showed that myocardial scintigraphy has a high negative predictive value in screening for significant CAV, its clinical significance in the screening for CAV following heart transplantation is controversial.[65,67-70] Puskas et al [68] showed in 43 patients that ^{201}Tl myocardial SPECT frequently revealed pathologic results in patients with normal coronary angiography and did not correlate with intimal thickening of epicardial coronary arteries accessible to intravascular ultrasonography in the early phase after transplantation. The authors concluded that the observed progressive scintigraphic abnormalities may be early signs of beginning graft vasculopathy, angiographically silent small vessel disease that is not necessarily correlated to IVUS findings in epicardial cornary arteries. Kerber et al[70] compared thallium SPECT with intravascular ultrasound imaging of coronary artery segments in 29 heart transplant recipients and showed that the extent of diffuse vessel wall alterations within the coronary arteries does not correlate with scintigraphic results.

2.1.2.3.2.Computed Tomography

Computed tomographic angiography has been newly introduced as an imaging modality for the prediction of CAV. Romeo et al[71] reported a sensitivity of 83% and a specificity of 95% for 16-slice multidetector CT (MDCT) for prediction of angiographic CAV and a negative predictive value of 95% in 53 heart transplant recipients. MDCT with adaptive multisegment reconstruction has shown a sensitivity and specificity of 86% and 99%, respectively.[72] Nunoda et al[73] showed a sensitivity of 90.0% and a specificity of 97.5% for 64-detector CT for diagnosing angiographic CAV. Iyengar et al[74] showed a good overall agreement between conventional X-ray coronary angiography and 64-slice MDCT.

The main concerns[71] with the routine use of MDCT after heart transplantation include the high heart rate of heart recipients which might compromise imaging quality, the size of the vessels, contrast media as a risk for worsening renal insufficiency, and radiation dose.

Coronary calcium has been shown by computed tomography to be a marker of CAV after heart transplantation.[75-77] Ludman et al[77] showed in 102 patients with a follow-up of a mean of 2.1 years that the absence of calcium had a negative predictive value of 87.5% with respect to angiographic CAV in any vessels. Knollmann et al[58] studied 112 heart transplant recipients and

reported a sensitivity of 94% and a specificity of 79%, when a calcium score of <55 was compared with >50% angiographic stenosis. With this threshold, EBCT had a negative predictive value of 99%, but a positive predictive value of 43%. The study showed also the association of EBCT total calcium with the degree of intimal proliferation. Ratliff et al[78] were unable to find a satisfactory correlation between EBCT calcium scores and angiographic results.

Myocardial perfusion reserve as detected by magnetic resonance imaging (MRI) after adenosine infusion has been shown to be an alternative to angiography for routine surveillance of CAV.[79] Magnetic resonance coronary angiography showed low sensitivity for detecting CAV.[80] Korosoglou et al[81] studied 69 consecutive heart transplant recipients with strain-encoded MRI. Strain-encoded MRI allowed differentiation of patients with versus those without CAV, as classified by coronary angiography. Peak systolic strain and strain rate were significantly reduced only in patients with severe CAV (stenosis ≥50%), while mean diastolic strain rate and myocardial perfusion reserve were already reduced in patients with normal vessels or stenosis < 50%. Myocardial perfusion reserve and mean diastolic strain rate had higher accuracy for the prediction of severe CAV (sensitivity: 100%, 100%, specificity: 82%, 87%,respectively) and followed peak systolic strain and strain rate (sensitivity: 86%,57%, specificity: 67%,91%, respectively).

Positron emission tomography (PET) has been considered the gold standard non-invasive method for myocardial perfusion imaging. The quantification of myocardial blood flow by PET showed to be significant in assessing the progression of CAV.[82-85]

2.2. Potential Usefulness of Myocardial Deformation Analysis for CAV Surveillance

2.2.1. Principle of Strain Imaging

Despite all obvious advantages, visual evaluation of ventricular wall motion by conventional echocardiography is very subjective and provides only semi-quantitative data. Furthermore, visual assessment has limited ability to detect more subtle changes in function and changes in timing of myocardial motion throughout systole and diastole. [86]

It is necessary to know the difference between myocardial wall motion and wall deformation. Wall motion is characterized by its velocity and displacement, whereas wall deformation can be described by strain and strain rate.[87] The concept of strain was initially introduced by Mirsky and Parmley.[88,89] The authors defined strain as a dimensionless quantity that describes the percent change in dimension from a resting state to one achieved following application of a force. Strain means deformation. Over time a moving object will change its position (displacement) but does not undergo deformation if all it parts move with the same velocity. When different parts of the object move with different velocities, the object will undergo deformation, resulting in change of shape. Thus wall motion measurements (displacement and velocity) cannot differentiate between active and passive movement of a myocardial segment, whereas deformation analyses (strain and strain-rate imaging) allow discrimination between active and passive myocardial tissue movement.[87]

Strain is a measure of how much an object has been deformed. The only possible deformation of an infinitesimally thin bar, one dimensional object, is lengthening or shortening and the amount of deformation, strain, can be defined by the formula[90]:

$\varepsilon = L - L_o/L_o = \Delta L/L_O$,

where ε is the symbol for strain, L is the current length after deformation and L_O is the original length.

When the length of the object is known during the deformation process, the instantaneous strain can be defined as follows[90]:

$\varepsilon = L(t) - L(t_o)/L(t_o)$,

where L(t) is the length at the time instance t and $L(t_o)$ is the initial length ($L(t_o) \equiv L_o$).The instantaneous deformation, called Lagrangian strain, is expressed relative to the initial length. The deformation can also be expressed relative to the length at a previous time instance as:

$d\varepsilon_N(t) = L(t+dt) - L(t)/L(t)$,

where dt is an infinitesimally small time interval and $d\varepsilon_N(t)$ is the infinitesimal amount of deformation occurring during dt. The total amount of strain can be calculated by integrating all the infinitesimal strain together, called natural strain :

$\varepsilon_N(t) = \int d\varepsilon_N(t)$.[90]

The Lagrangian and natural strain are approximately equal in small deformations, but the difference between the Lagrangian and natural strain becomes significant in the large deformations, which occur in the cardiac systole and diastloe.[90]

The extent of deformation (strain) is expressed as a percentage. Negative strain implies shortening of a segment and positive strain lengthening of a segment related to its original length. Myocardial contraction can be described by radial thickening (positive strain) and circumferential shortening (negative strain) in parasternal short-axis views, and longitudinal shortening (negative strain) in apical views.

Strain rate (Sr) is a rate of deformation and its symbol is έ with the unit 1/sec:

$\acute{\varepsilon} = \Delta\varepsilon/\Delta t = (\Delta L/L_0)/\Delta t = (\Delta L/\Delta t)/ L_0 = \Delta V/L_o$,

where ΔV is the velocity gradient between two adjacent points.[87]

In the cardiac systole, the apical parts of the ventricle pull down the ventricular base with the wall motion velocity and wall displacement increasing from apex to base and the motion of the base is partly an effect of apical contraction – tethering, suggesting that even completely passive segments can show motion without deformation.[91]

Myocardial deformation is more constant along the ventricular wall (position independent if the velocity gradient is evenly distributed) and is more suitable than wall motion analysis (velocity and displacement) for prediction of regional myocardial dysfunction.[91,92] Strain and Sr are not measurements of contractility because deformation is load dependent.[87]

Tissue Doppler-Derived Strain and Strain Rate

As mentioned above, the myocardial velocity gradient over a distance ($\Delta V/L_o$) is equivalent to the change of strain over time ($\Delta\varepsilon/\Delta t$), namely έ. Temporal integration of the velocity gradient provides the logarithmic strain estimate, natural strain, named from the use of the natural logarithm. This is the theoretical basis for measuring strain by TDI.[86]

The main limitations of strain and Sr by TDI are signal noise and angle dependency.[90] Sr by TDI has significant problems with random noise, an effect of measuring the difference between velocities because the error is the sum of the errors of the two velocities. This can be improved by increasing the sample distance but at the cost of lower temporal and spatial resolution. Angle dependency affects Sr measurements significantly. Myocardial velocity is reduced in proportion

to the cosine of the angle between the direction of myocardial movement and the ultrasound beam. TDI assesses tissue movement in relation to the transducer rather than relative to adjacent segments, which can affect tissue Doppler derived strain and strain rate imaging. TDI-derived strain and strain rate measurements are not highly reproducible (more than 10-15% interobserver variability).[87]

Speckle Tracking Derived Strain Imaging

Speckle tracking echocardiography (STE) measures strain by tracking speckles in gray scale echocardiographic images. The speckles, black and white ¨image-data-particles˝, are created by interference of ultrasound beams (US) in the myocardium and are seen in gray scale B-mode images as a characteristic speckle pattern[86] (Figure 2).

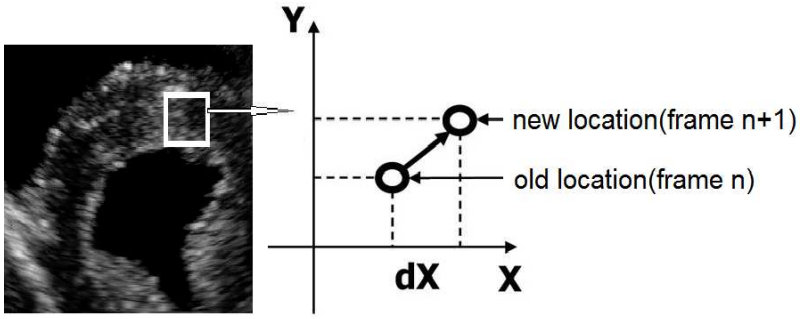

Figure 2. real-time tracking of a speckle on gray scale B-mode echocardiographic image frame to frame by software.

The speckles are the result of constructive and destructive interference of US back-scattered from structures smaller than a wavelength of US.[86]

The speckles function as natural acoustic markers, which are tracked from frame to frame. These speckles are statistically equally distributed throughout the myocardium. The size of these markers is 20 to 40 pixels. Unlike TDI strain imaging, STE analyzes Lagrangian strain. Special software allows spatial and temporal image analysis with recognition and selection of the speckles on grey scale echocardigraphic images. The geometric shift of each speckle represents local tissue movement. When frame rate is known, the change in speckle position allows calculation of its velocity. By tracking the speckles, strain and Sr can be calculated. The advantage of non-Doppler 2D-strain imaging is angle independence, because it tracks in two dimensions, along the direction of the wall, not along the ultrasound beam.[93]

It is necessary to know that different tracking softwares may result in different results.[87] The necessity of high image quality is a major limitation of STE for routine clinical applicability in all patients.[93,94]

The intraobserver and interobserver variability of STE were found to be low: 3.6% to 5.3% and 7% to 11.8%, respectively.[93]

2.2.2. Clinical Usefulness of Strain Imaging

Echocardiographic strain imaging is a promising tool for the evaluation of myocardial function. The clinical applications of strain imaging are increasing and provide incremental diagnostic and prognostic value over standard 2D and Doppler echocardiography. This is due its ability to discriminate between active and passive movement of myocardial segments, to quantify intraventricular dyssynchrony and to evaluate components of myocardial function, such as longitudinal myocardial shortening, that are not visually assessable.[87]

Because longitudinal mechanics predominate in the ischemia-vulnerable subendocardium and strain imaging analyzes the longitudinal component of deformation, strain imaging is suitable to assess myocardial ischemia. Several studies reported a reduction of strain and strain rate values in visually normokinetic segments supplied by stenotic arteries[95], the diagnostic value of strain-identified regional post-ischemic dysfunction in patients with chest pain in whom the ECG has normalized[96], and the potential of early diastolic deformation to improve diagnostic accuracy.[97] A progressive impairment of 2D global strain and Sr was directly related to increasing severity of coronary disease in patients with normal ejection fraction.[98] Strain imaging, as an adjunct to dobutamine stress echocardiography (DSE), improved the diagnostic accuracy of DSE for detecting CAD.[99-103] Longitudinal strains are reduced in patients with myocardial infarctions[104] and correlate with infarct size and ejection fraction[105,106] and predict LV remodelling and clinical events.[107] Strain imaging showed its usefulness in identifying viable myocardium.[108-110]

Strain and strain rate measurements have been found to be sensitive indications for sub-clinical diseases, including diabetes, systemic sclerosis, arterial hypertension, mitral regurgitation, aortic regurgitation and non-ischemic cardiomyopathies.[111-117]

Cardiac resynchronization therapy (CRT) has made a large impact on improving symptoms and survival in heart failure patients. Strain imaging allows reliable determination of cardiac timing intervals, which is useful in assessing LV intraventricular mechanical dyssynchrony and has proved to be useful for both the selection of patients who might benefit from CRT and the evaluation of CRT efficiency.[118-120]

In patients with idiopathic dilated cardiomyopathy and similar LVEF who were accepted for heart transplantation, those with rapid worsening toward inotropic support dependence showed higher dyssynchrony and lower global strain rate values than those who remained clinically stable.[121]

In patients with left ventricular assist devices (LVAD), 2D-strain imaging proved to be useful in evaluating cardiac recovery during mechanical unloading, decision for weaning from LVAD and follow-up after LVAD explantation.[87]

The assessment of diastolic function by 2D-strain imaging was shown to be useful for the evaluation of patients referred for heart transplantation.[122] Late diastolic strain rate and the diastolic E/A strain rate ration showed high predictive values for the outcome of patients with idiopathic dilated cardiomyopathy during the first 6 months after listing for heart transplantation.

Strain imaging in heart transplantation

Several studies showed that strain and strain rate imaging are of clinical value in cardiac rejection surveillance.

Pieper et al[123] studied an experimental rat transplant model with speckle tracking 2-dimensional strain echocardiography (2DSE). Despite grade 3B rejection in allografts and no rejection in isografts, there was no difference between isografts and allografts in fractional shortening or ejection fraction. However, 2DSE revealed decreases between isografts and allografts in global radial strain, peak radial systolic strain rate, and peak circumferential systolic strain rate. They also showed differences not only in systolic strain but also in the early diastolic strain rate between allograft and isograft hearts. Analysis of longitudinal strain and strain rate imaging was not done for technical reasons.

Eroglu et al[124] studied 57 “normal” heart transplant recipients (age 36±12 years; post-HTx 5.5±3 years), who have a normal ECG with a ORS duration of less than 120ms, a normal LVEF, non-significant TR, and a cardiac biopsy ≤ ISHLT Grade 1A. They also had a normal invasive measurement of right heart pressures as well as normal coronary angiography, which is defined as <50% focal stenosis and/or more than mild distal vessel attenuation, with color Doppler myocardial imaging. They reported normal values for both radial and longitudinal regional peak systolic velocity, which is highest at the base and decreases as the sample volume is moved apically, and strain and strain rate, which was homogenous in the septum, lateral, anterior, and

inferior wall. In the two patients (not included in normal HTx group) with 1B biopsy results, radial strain and strain rate values were significantly reduced in the posterior wall when compared to normal HTx values. The authors reported also 4 patients with severe heart transplant vasculopathy, who had normal global systolic function but decreased strain and strain rate values ($p < 0.005$ vs normal HTx).

In a prospective study of 31 consecutive heart transplant patients, Marciniak et al[125] showed that a significant reduction in peak systolic strain and strain rate in both radial and longitudinal deformation could be detected in early rejection grades. Radial strain for left ventricular posterior wall $\leq 30\%$ predicted rejection $\geq$IB with a sensitivity of 85%, a specificity of 90% and a negative predictive value of 93%. A cut-off value of Sr $<3.0\ s^{-1}$ had a sensitivity of 80%, a specificity of 86% and a negative predictive value of 89% for acute rejection. Kato et al[126] reported in 35 transplant recipients a predictive accuracy of 82.3% of a systolic strain cut-off value of -27.4% for acute rejection $\geq$ IB, which increased to 84.8% with the combination of systolic strain and diastolic strain rate. Dandel et al[127] showed that a sudden decrease of more than 15% of the radial global strain in patients with stable or reduced blood pressure was very highly predictive of acute rejection.

Saleh et al[128] evaluated strain and strain rate in 40 heart transplant recipients at 1 year after transplant, who had no histologic evidence of severe rejection (Grade 2R or higher), LVEF $\geq$55%, no severe valvular disease, and no significant CAV, with STE using velocity vector imaging. They reported normal values for global longitudinal strain, strain rate and the standard deviation of the global longitudinal strain time to peak as a synchrony parameter:13.43%±2.39%, -0.83±0.15 s^{-1}, and 41.67±13.53ms, respectively.

Syeda et al[129] studied 31 heart transplant recipients with 10.6 years post-transplantation with STE and multislice computed tomographic coronary angiography (MSCTA). They showed that even though "healthy" transplant recipients without CAD exhibit normal global systolic function as assessed by conventional methods, deformation indices are altered when compared with those of control subjects.

Eroglu et al[130] studied 50 patients at 6 years post-transplantation with dobutamine stress echocardiography using color myocardial Doppler velocity. Peak systolic longitudinal strain rate response $<0.5\ s^{-1}$ during DSE identified patients with CAV (mild and severe) with a sensitivity of 88%, specificity of 85% and a negative predictive value of 92%.

To our knowledge, there is so far no study, that has assessed the usefulness of speckle tracking echocardiography in the prediction of CAV.

3. Study

3.1. Objective

The aim of this study was to assess the reliability of STE in distinguishing between patients with and without CAV and to search for parameters with sufficient sensitivity and specificity to allow early recognition of functional myocardial alterations induced by focal coronary stenoses, before any appearance of visually detectable changes in cardiac function. The final goal was to evaluate the potential usefulness of STE to optimize the timing of coronary angiographies after HTx.

3.2. Methods

3.2.1. Patients and Study Design

We selected for evaluation all consecutive heart transplanted adult patients with normal LVEF and lack of visible regional wall motion alterations during conventional echocardiography who underwent coronary angiography between 2005 and 2010. In this period before each heart catheterization a comprehensive echocardiographic examination, including STE, was performed. Routine coronary angiographies were performed in these patients annually or at a longer time interval of up to 2 years, depending on renal function and other acute or chronic diseases. Additional angiographies were performed whenever CAV or the progression of known CAV was suspected clinically (arrhythmias, clinical symptoms) or by ECG, electron beam tomography and/or PW-TDI changes.[57] STE was not used for the decision making in favor of or against the coronary angiographies. Echcardiography including STE was performed in all patients before the coronary angiography on the same day.

Criteria for exclusion from the study were acute rejection, donor-transmitted coronary artery disease, bundle branch block, LV ejection fraction <55% and visible regional wall motion abnormalities during conventional echocardiography. Also patients with poor echocardiographic image quality even in only one myocardial segment were excluded from the study if the computer signaled that reliable deformation analyses would not be possible in that particular segment.

A total of 202 heart transplant recipients fulfilled these criteria and were included in the study.

3.2.2. Echocardiographiy

3.2.2.1. Conventional Echocardiography

Echocardiography was performed using a Vivid 7 ultrasound system (General Electric) and 2.5MHz transducer. Interventricular septum (IVS) thickness, left ventricular internal dimension in diastole and systole ($LVID_{d,s}$), and LV posterior wall (PW) thickness, were measured by M-mode or B-mode. The LV ejection fraction was calculated by the Simpson method. Pulse-wave Doppler echocardiography was performed, and peak early (E) and late (A) transmitral filling velocities, deceleration time (DT) of E, and isovolumic relaxation time (IVRT) were measured from mitral inflow velocities with calculation of the ratio (E/A).

3.2.2.2. Speckle-tracking Echocardiography

Echocardiographic images were acquired in the parasternal short-axis views at the level of mitral valve (SAX), apical long-axis (APLAX), two-chamber (2CH), and four-chamber (4CH) views.

A sector scan angle of 30^o to 60^o was chosen, and frame rates of 50 to 70 Hz were used. Data were stored at the same frame rate as the acquisition frame rate and transferred to a workstation for off-line analysis. Offline speckle-tracking analysis was performed by the software for echocardiographic quantification (EchoPAC version 7, GE Vingmed Ultrasound AS USA). Endomyocardial borders of the LV were manually traced using a point-and-click technique at the end-systolic frame and epicardial tracing was automatically performed by the computer algorithm and, when necessary, manually adjusted to cover the whole myocardial wall. The tracking algorithm then followed the myocardial speckles during the cardiac cycle. Tracking was accepted only if both visual inspections as well as the EchoPAC software indicated adequate tracking. The software automatically divided the cross-sectional image into six segments according to an 18-segment model of the LV, as recommended by the American Heart Association. The LV segments to be analyzed were the basal, middle, and apical segments of the septum and the lateral wall in 4CH, the anterior and inferior wall in 2CH, and the anteroseptal and posterior wall in APLAX, as well as the anteroseptal, anterior, lateral, posterior, inferior, and septal segments in SAX. Myocardial longitudinal, radial, and circumferential strain and SR were obtained in each segment. Global strain and Sr were averages of the strain and Sr values of six segments in SAX, APLAX, 2CH, and 4CH, respectively.

The reproducibility of the measurements was tested by 2 examiners in 15 patients.

Duration of a complete measurement for STE parameters was tested by an experienced examiner in 10 patients.

The strain and strain rate parameters can be divided into the timing and magnitude parameters.[94] The following parameters were obtained (figure 3, 4):

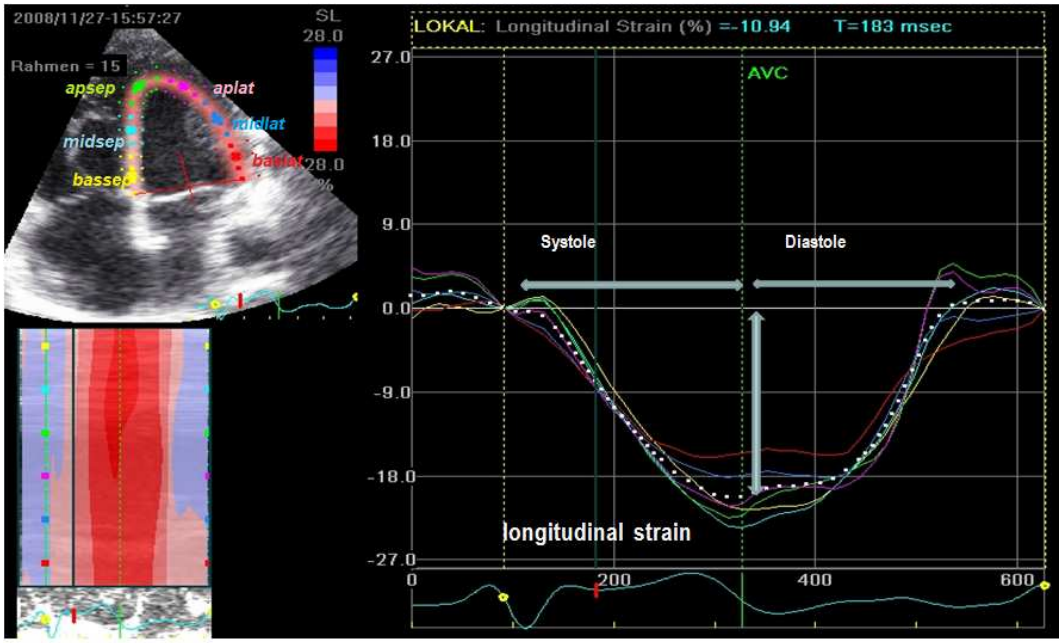

Figure 3. Curves of strain in 6 segments (4CH)

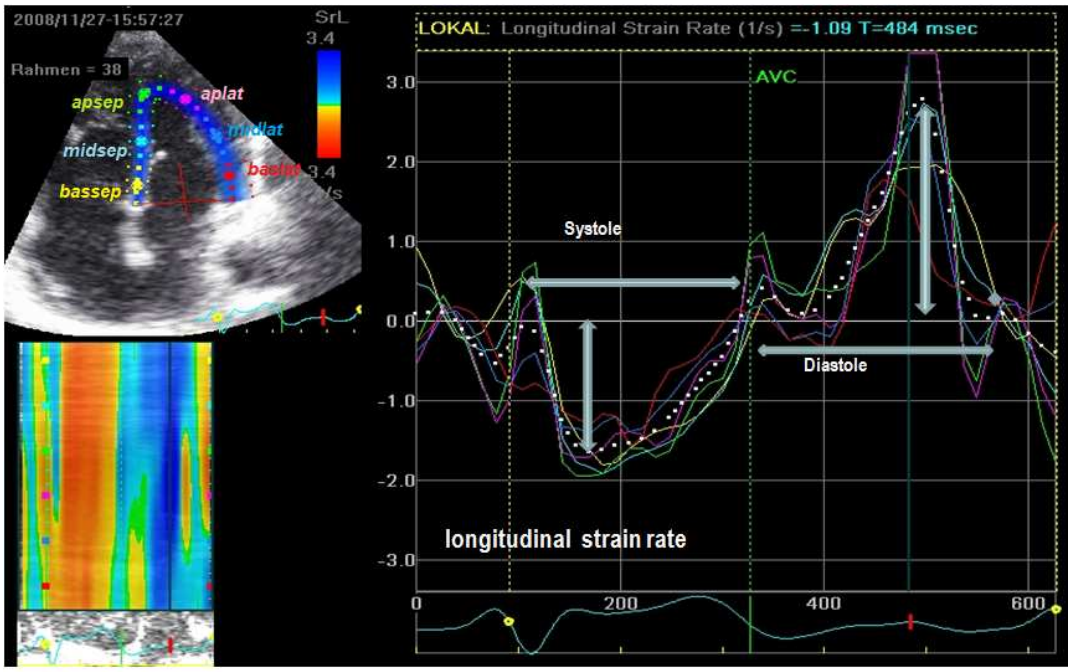

Figure 4. Curves of strain rate in 6 segments (4CH)

∆ Strain parameters

1. global peak systolic strain (GS), defined as the mean value of peak systolic strains of each of the 6 segments

2. peak systolic strain dispersion ($S_{disp.}$), defined as the difference between maximal and minimal strain in each of the 6 segments

3. peak systolic strain relative dispersion ($S_{disp.}(r)$), defined as the peak systolic strain dispersion divided by the global peak systolic strain

∆ SR parameters

1. global peak systolic strain rate (GSr), defined as the mean value of peak systolic Srs of each of the 6 segments

2. time to peak systolic strain rate (TpSr), defined as the time interval from R wave on the electrocardiogram to the global peak systolic Sr

3. acceleration of systolic deformation (GSr/TpSr), defined as the global peak systolic strain rate divided by the time to peak systolic strain rate

4. early and late global diastolic strain rate (GSr_E and $GSr_{A,}$ respectively) and GSr_E/GSr_A ratio

5. time to peak early global diastolic strain rate ($TpSr_E$), defined as the time interval from aortic valve closure to the peak early global diastolic strain rate (GSr_E)

6. acceleration of early diastolic deformation (GSr_E / $TpSr_E$)

∆ Synchrony parameters

1. dispersion of time to peak systolic strain ($TpS_{disp.}$), defined as the time difference between the maximal and the minimal time to peak systolic strain in 6 each segments

2. one standard deviation of the time to peak systolic strain (SD_{TpS})

3. intraventricular asynchrony index ($Index_{asynch.}$), defined as the standard deviation of the time to peak systolic strain divided by averaged time to peak systolic strain

3.2.3. Cardiac catheterization

After standard hemodynamic recordings, biplanar angiograms were acquired digitally and by cine film on standard biplanar angiographic x-ray equipment (INTEGRIS/LARC system Philips). Angiographic evaluation of CAV was based on Stanford criteria[7] (Figure 5).

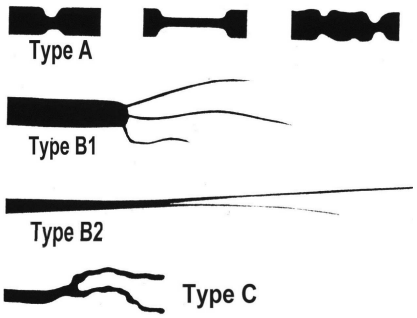

Figure 5. Stanford clssification

For analysis, heart transplant recipients were divided into three groups: group 1 consisted of patients with no angiographic CAV; group 2, patients with type B and no type A lesions, and group 3, patients with type A, defined as focal stenosis ≥50%, and type B lesions. The patients who had type C lesions also had type B or type A and were included in group 2 or group 3, depending on whether the lesions were of type A or type B.

3.2.4. Statistics

Statistical analysis was performed using commercially available software (SPSS, version 19.0 for windows) and all data are presented as mean ± one standard deviation.

Differences in all parameters were evaluated using an unpaired two-sided t-test. Receiver operating characteristics (ROC) were used to determine the diagnostic value of strain and Sr parameters for the prediction of CAV. Differences were considered significant at $p < 0.05$.

3.3. Results

3.3.1. Coronary angiography

The coronary angiogram was normal in 56 (27.7%) patients (group1). Coronary artery disease was present in the other 146 patients. 87 (43.1%) patients had CAV with diffuse type B lesions but no focal stenosis (group2) and 59 (29.2%) patients with diffuse type B lesions and focal stenosis. The clinical characteristics and hemodynamic data are given in table 1 and 2.

Table 1. Clinical characteristics

	Group 1 (n = 56)	Group 2 (n = 87)	Group 3 (n = 59)	P value	
				1:2	2:3
Age at transplant, years	43 ± 13	45 ± 14	45 ± 14	0.310	0.953
Age at examination, years	44 ± 13	53 ± 14	56 ± 13	0.000	0.209
Post-transplant time, years	1.0 ± 2.3	7.9 ± 4.3	10.4 ± 5.6	0.000	0.001
Height, m	174.8 ± 9.7	174.3 ± 9.6	174.2 ± 7.8	0.761	0.984
Weight, kg	77.3 ± 14.4	82.6 ± 1.8	81.5 ± 18	0.047	0.724
BSA, m^2	1.9 ± 0.2	2.0 ± 0.2	2.0 ± 0.2	0.179	0.800
BMI, kg/m^2	25.3 ± 4.4	27.1 ± 4.7	26.8 ± 5.4	0.020	0.725

The mean age at transplantation did not significantly differ between the groups. The posttransplant time increased significantly with increased severity of angiographic lesions. The weight and BMI (body mass index) were significantly lower in group 1 than in group 2 and 3.

Table 2. Hemodynamic data

	Group 1 (n = 56)	Group 2 (n = 87)	Group 3 (n = 59)	P value	
				1:2	2:3
HR, bpm	88 ± 10	87 ± 13	87± 12	0.199	0.085
SBP_{aortic} , mmHg	130 ± 20	134 ± 23	141 ± 22	0.273	0.060
DBP_{aortic} , mmHg	78 ± 12	79 ± 14	80 ± 12	0.604	0.468
LVEDP, mmHg	13.6 ± 5.2	14.6 ± 4.6	16.7 ± 5.8	0.263	0.027
PA (mean), mmHg	18.5 ± 4.5	19.9 ± 5.2	22.4 ± 6.1	0.098	0.015
RA (mean), mmHg	6.6 ± 3.9	7.2 ± 3.5	8.8 ± 3.7	0.371	0.009
CI, $l\ min^{-1}\ m^{-2}$	3.4 ± 0.6	3.3 ± 0.9	3.1 ± 0.8	0.408	0.242

The heart rate, diastolic blood pressure (DBP_{aortic}) and cardiac index (CI) did not differ significantly between the 3 groups. None of the hemodynamic parameters studied differed significantly between group 1 and group 2. Mean pulmonary artery pressure (PA mean), mean right atrial pressure (RA mean) and left ventricular end-diastolic pressure (LVEDP) were significantly higher in group 3 than in group 1 and 2.

3.3.2. Echocardiographic Examination

3.3.2.1. Conventional Echocardiographic Examination

3.3.2.1.1. Conventional Echocardiographic Parameters

Conventional M-mode and Doppler echocardiographic parameters are given in Table 3 and 4.

Table 3. Conventional M-/B-mode echocardiographic parameters

	Group 1 (n = 55)	Group 2 (n = 85)	Group 3 (n = 59)	P value	
				1:2	2:3
$LVID_d$, cm	4.6 ± 0.5	4.8 ± 0.4	4.9 ± 0.5	0.006	0.354
$LVID_s$, cm	2.8 ± 0.5	2.9 ± 0.4	3.0 ± 0.4	0.111	0.050
IVS, cm	1.07 ± 0.10	1.07 ± 0.11	1.15 ± 0.09	0.922	0.000
PW, cm	1.05 ± 0.11	1.07 ± 0.10	1.11 ± 0.09	0.317	0.026
EF, %	70.9 ± 7.1	70.5 ± 5.9	68.4 ± 5.8	0.690	0.039
FS, %	40.1 ± 6.9	40.2 ± 5.0	38.4 ± 4.6	0.900	0.031

The left ventricular internal diameter in diastole ($LVID_d$) was significantly greater in group 2 and 3 than in group 1. The ejection fraction and fractional shortening of left ventricle did not differ significantly between group 1 and group 2, but appeared to be significantly higher than in group 3. The interventricular septum and posterior wall thickness were significantly greater in group 3 than in group 1 and 2.

Table 4. Conventional Doppler echocardiogrphic parameters

	Group 1 (n = 45)	Group 2 (n = 71)	Group 3 (n = 50)	P value	
				1:2	2:3
E, cm/s	92.0 ± 22.8	88.3 ± 23.0	89.6 ± 20.2	0.399	0.732
A, cm/s	40.4 ± 12.5	42.0 ± 12.7	37.3 ± 8.7	0.491	0.016
E/A	2.5 ± 0.9	2.2 ± 0.8	2.5 ± 0.8	0.162	0.042
DT, ms	127.9 ± 36.4	115.0 ± 16.4	112.0 ± 15.5	0.029	0.307
IVRT, ms	67.0 ± 11.0	64.3 ± 7.7	62.2 ± 8.7	0.107	0.139

The deceleration time of E wave (DT) in mitral inflow appeared to be significantly shorter with increased severity of angiographic lesions. The transmitral A wave velocity was significantly lower, with the ratio of transmitral velocities (E/A) higher, in group 3 than in group 1 and 2 .

3.3.2.1.2. Diagnostic value of conventional echocardiographic parameters for CAV

We selected the conventional echocardiographic parameters, that were found to differ significantly between the groups, and used the ROC to determine their diagnostic value for CAV (table 5, 6).

Table 5. The ROC analysis of conventional echocardiographic parameters for prediction of CAV with no focal stenosis (Group 1:2)

	AUC(%)	95% CI	Cut-off	Sensitivity(%)	Specificity(%)
$LVID_d$, cm	63.7	0.54-0.73	≥4.7	65.9	61.8
DT, ms	61.0	0.49-0.73	≤118	60.6	60.0

Table 6. The ROC analysis of conventional echocardiographic parameters for prediction of CAV with focal stenosis (Group 2:3)

	AUC(%)	95% CI	Cut-off	Sensitivity(%)	Specificity(%)
EF, %	58.8	49.3-68.3	≤68.5	52.5	59.5
FS, %	59.3	49.8-68.8	≤38.5	57.6	58.3
A, cm/s	60.8	50.8-70.9	≤39.5	68.0	59.2
E/A	62.6	52.6-72.6	≥2.1	64.0	56.3

3.3.2.2. Speckle tracking parameters

We divided the speckle tracking parameters into strain, Sr, and synchrony parameters and analyzed each of the parameters in SAX, 4CH, APLAX, and 2CH, respectively .

Observer agreements and Duration of parameter measurement:

The intra- and interobserver variabilities were 5% and 8% for global peak systolic strain, and 7% and 10% for global peak systolic strain rate, respectively.

The average duration of STE evaluation by an experienced examiner was 5 min per patients.

3.3.2.2.1. Strain parameters

The radial global peak systolic strain (GS) did not significantly differ between group 1 and 2, but it was significantly greater in groups 1 and 2 than in group 3. Radial peak systolic strain

relative dispersion ($S_{disp.}(r)$) was significantly higher in patients with more severe angiographic lesions (table 7).

Table 7. Radial peak systolic strain and derived parameters (%)

	Group 1 (n=45)	Group 2 (n=69)	Group 3 (n=42)	P value	
				1:2	2:3
Antero-septal	41.4 ± 13.4	38.3 ± 12.7	29.5 ± 12.4	0.319	0.000
Anterior	42.4 ± 14.1	38.6 ± 12.1	29.7 ± 11.2	0.145	0.000
Lateral	44.5 ± 14.9	40.7 ± 12.6	31.7 ± 13.1	0.167	0.001
Posterior	46.0 ± 13.3	46.6 ± 14.4	34.3 ± 15.4	0.834	0.000
Inferior	44.2 ± 12.7	45.6 ± 14.5	33.1 ± 14.4	0.564	0.000
Septal	41.9 ± 12.7	41.1 ± 13.6	30.9± 13.4	0.724	0.000
GS	43.4 ± 12.8	41.8 ± 11.9	31.5 ± 11.8	0.832	0.000
$S_{disp.}$	11.1 ± 7.0	15.7 ± 10.1	15.6 ± 8.6	0.006	0.988
$S_{disp.}(r)*100$	27.1 ± 16.9	38.4 ± 25.4	53.4 ± 30.7	0.005	0.010

The circumferential global peak systolic strain (GS) was significantly reduced and the circumferential peak systolic strain relative dispersion ($S_{disp.}(r)$) significantly increased with increased severity of angiographic lesions (table 8).

Table 8. Circumferential peak systolic strain and derived parameters (%)

	Group 1 (n=45)	Group 2 (n=69)	Group 3 (n=42)	P value	
				1:2	2:3
Antero-septal	-24.2 ± 4.5	-22.6 ± 5.5	-19.9 ± 5.8	0.088	0.021
Anterior	-19.2 ± 5.6	-17.6 ± 5.5	-13.2 ± 6.7	0.134	0.001
Lateral	-15.4 ± 5.4	-11.5 ± 6.9	-7.8 ± 6.3	0.001	0.005
Posterior	-17.9 ± 5.2	-12.5 ± 6.2	-10.8 ± 5.9	0.000	0.169
Inferior	-23.2 ± 5.4	-17.7 ± 6.4	-15.4 ± 7.0	0.000	0.076
Septal	-24.9 ± 4.8	-21.8 ± 5.2	-18.8 ± 5.6	0.002	0.006
GS	-20.8 ± 3.5	-17.3 ± 3.7	-14.3 ± 4.1	0.000	0.000
$S_{disp.}$	12.3 ± 6.2	14.8 ± 7.1	16.4 ± 5.4	0.053	0.169
$S_{disp.}(r)*100$	-60.8 ± 3.5	-89.2± 44.2.	-129.8 ± 88.9	0.000	0.008

Table 9. Longitudinal peak systolic strain and derived parameters in 4 CH (%)

	Group 1 (n=56)	Group 2 (n=87)	Group 3 (n=59)	P value	
				1:2	2:3
Septum					
Basal	-17.5 ± 2.8	-15.8 ± 3.7	-12.1 ± 4.0	0.003	0.000
Mid	-18.5 ± 3.1	-17.4 ± 3.7	-14.0 ± 4.0	0.059	0.000
Apical	-20.3 ± 4.3	-19.6 ± 4.9	-15.2 ± 6.3	0.419	0.000
Lateral wall					
Apical	-21.3 ± 4.5	-19.7 ± 6.7	-14.7 ± 6.8	0.090	0.000
Mid	-18.8 ± 3.3	-17.7 ± 4.0	-13.6 ± 5.2	0.063	0.000
Basal	-17.4 ± 3.0	-16.2 ± 3.9	-14.0 ± 5.3	0.047	0.006
GS	-19.0 ± 2.8	-17.7 ± 3.0	-13.9 ± 3.2	0.014	0.000
$S_{disp.}$	6.4 ± 3.5	8.7 ± 4.1	11.4 ± 4.0	0.001	0.000
$S_{disp.}(r)*100$	-33.9 ± 14.9	-48.5 ± 19.6	-86.5 ± 42.2	0.000	0.000

Global peak systolic strain (GS) was significantly increased and peak systolic strain dispersion ($S_{disp.}$) and peak systolic strain relative dispersion ($S_{disp.}(r)$) were also significantly increased with increased severity of angiographic lesions.

Table 10. Longitudinal peak systolic strain and derived parameters in APLAX (%)

	Group 1 (n=56)	Group 2 (n=86)	Group 3 (n=57)	P value	
				1:2	2:3
Posterior wall					
Basal	-18.2 ± 3.5	-16.7 ± 4.2	-14.9 ± 6.4	0.024	0.069
Mid	-18.6 ± 3.6	-17.2 ± 4.1	-15.1 ± 5.8	0.035	0.023
Apical	-21.5 ± 3.9	-20.4 ± 5.1	-16.7 ± 6.3	0.189	0.000
Anterior septum					
Apical	-21.0 ± 4.6	-20.1 ± 5.6	-16.4 ± 7.0	0.289	0.001
Mid	-18.7 ± 3.9	-17.8 ± 4.1	-14.2 ± 5.5	0.155	0.000
Basal	-17.8 ± 3.3	-16.3 ± 3.6	-12.4 ± 5.0	0.015	0.000
GS	-19.3 ± 3.1	-18.1 ± 3.4	-15.0 ± 3.6	0.032	0.000
$S_{disp.}$	6.6 ± 2.9	8.5 ± 4.0	12.4 ± 5.8	0.002	0.000
$S_{disp.}(r)*100$	-33.7 ± 13.1	-46.1 ± 18.6	-84.8 ± 42.5	0.000	0.000

Global peak systolic strain (GS) was significantly increased and peak systolic strain dispersion ($S_{disp.}$) and peak systolic strain relative dispersion ($S_{disp.}(r)$) were also significantly increased with increased severity of angiographic lesions.

Table 11. Longitudinal peak systolic strain and derived parameters in 2 CH (%)

	Group 1 (n=46)	Group 2 (n=33)	Group 3 (n=40)	P value	
				1:2	2:3
Inferior wall					
Basal	-17.7 ± 3.2	-16.6 ± 3.1	-13.5 ± 5.6	0.147	0.004
Mid	-17.9 ± 3.4	-16.8 ± 2.8	-14.9 ± 5.2	0.143	0.041
Apical	-19.6 ± 4.2	-19.0 ± 3.9	-16.7 ± 6.2	0.558	0.051
Anterior wall					
Apical	-20.1 ± 4.7	-20.3 ± 4.9	-14.7 ± 6.2	0.843	0.000
Mid	-18.9 ± 3.6	-18.7 ± 4.2	-13.1 ± 5.7	0.849	0.000
Basal	-18.0 ± 3.0	-17.2 ± 4.1	-12.7 ± 6.6	0.355	0.001
GS	-18.7 ± 2.9	-18.1 ± 2.7	-14.3 ± 3.6	0.388	0.000
$S_{disp.}$	6.1 ± 3.1	7.4 ± 3.1	12.4 ± 5.3	0.071	0.000
$Rel.S_{disp.*}100$	-32.5 ± 15.7	-40.5 ± 15.6	-90.7 ± 39.5	0.029	0.000

Global peak systolic strain and peak systolic strain dispersion ($S_{disp.}$) did not differ significantly between group 1 and 2, but were significantly greater than in group 3. The peak systolic strain relative dispersion ($S_{disp.}(r)$) showed a significant increase with increased severity of angiographic lesions.

We compared the longitudinal strain parameters in each longitudinal view to each other within each group. No significant difference in the longitudinal strain parameters, except in $S_{disp.}(r)$ in group 2, was found within each group (table 12).

Table 12. Longitudinal peak systolic strain and derived parameters in each group (%)

	4CH	APLAX	2CH	P value		
				4CH:APLAX	4CH:2CH	APLAX:2CH
Group 1						
GS	-19.0 ± 2.8	-19.3 ± 3.1	-18.7 ± 2.9	0.564	0.614	0.313
$S_{disp.}$	6.4 ± 3.5	6.6 ± 2.9	6.1 ± 3.1	0.802	0.586	0.395
$S_{disp.}(r)_{*}100$	-33.0 ± 14.9	-33.7 ± 13.1	-32.5 ± 15.7	0.793	0.872	0.683
Group 2						
GS	-17.7 ± 3.0	-18.1 ± 3.4	-18.1 ± 2.7	0.492	0.520	0.951
$S_{disp.}$	8.7 ± 4.1	8.5 ± 4.0	7.4 ± 3.1	0.671	0.055	0.118
$S_{disp.}(r)_{*}100$	-48.5 ± 19.6	-46.1 ± 18.6	-40.5 ±15.6	0.417	0.022	0.099
Group 3						
GS	-13.9 ± 3.2	-15.0 ± 3.6	-14.3 ± 3.6	0.114	0.646	0.358
$S_{disp.}$	11.4 ± 4.0	12.4 ± 5.8	12.4 ± 5.3	0.279	0.305	0.989
$S_{disp.}(r)_{*}100$	-86.5 ± 42.2	-84.8 ± 42.5	-90.7 ± 39.5	0.831	0.615	0.486

3.3.2.2.2. Strain rate parameters

Table 13. Radial Sr and derived parameters

	Group 1 (n=45)	Group 2 (n=69)	Group 3 (n=42)	P value	
				1:2	2:3
GSr , s^{-1}	1.9 ± 0.4	2.0 ± 0.5	1.7 ± 0.6	0.574	0.002
TpSr, ms	119.4 ± 23.9	160.6 ± 35.4	163.2 ± 33.0	0.000	0.699
GSr/TpSr, ms^{-2} *100	1.7 ± 0.5	1.3 ± 0.5	1.1 ± 0.5	0.000	0.009
GSr_E, s^{-1}	-2.3 ± 1.0	-2.1 ± 0.8	-1.9 ± 0.8	0.439	0.165
GSr_A, s^{-1}	-0.8 ± 0.4	-0.7 ± 0.3	-0.5 ± 0.3	0.180	0.001
GSr_E/GSr_A	4.1 ± 3.2	5.1 ± 7.1	5.8 ± 4.0	0.353	0.509
$TpSr_E$, ms	119.8 ± 34.4	131.6 ± 42.8	105.9 ± 37.6	0.108	0.01
$GSr_E/TpSr_E$, ms^{-2} *100	-2.1 ± 1.0	-1.9 ± 1.2	-2.0 ± 0.9	0.336	0.524

Global peak systolic strain rate (GSr) did not differ significantly between group 1 and 2, but was significantly higher than in group 3. The time to peak systolic strain rate (TpSr) was significantly longer in group 2 than in group 1, but not significantly different between group 2 and 3. The

acceleration of systolic deformation (GSr/TpSr) was significantly reduced with increased severity of angiographic lesions.

No studied radial diastolic Sr parameters showed a significant difference between group 1 and 2, but the late global diastolic Sr (GSr_A) and time to peak early diastolic Sr ($TpSr_E$) appeared to be significantly lower in group 3 than group 1 and 2 (table 13).

Table 14. Circumferential Sr and derived parameters

	Group 1 (n=45)	Group 2 (n=69)	Group 3 (n=42)	P value	
				1:2	2:3
GSr, s^{-1}	-1.6 ± 0.4	-1.3 ± 0.3	-1.0 ± 0.3	0.000	0.000
TpSr, ms	116.5 ± 20.9	154.8 ± 26.2	156.1 ± 24.7	0.000	0.794
GSr/TpSr, ms^{-2} *100	-1,4 ± 0.5	-0.8 ± 0.2	-0.7 ± 0.2	0.000	0.000
GSr_E, s^{-1}	1.9 ± 0.6	1.7 ± 0.5	1.4 ± 0.4	0.032	0.051
GSr_A, s^{-1}	0.6 ± 0.4	0.4 ± 0.3	0.2 ± 0.2	0.013	0.009
GSr_E/GSr_A	5.7 ± 4.6	8.0 ± 8.8	10.8 ± 9.8	0.063	0.132
$TpSr_E$, ms	120.1 ± 41.8	122.8 ± 37.8	122.0 ± 37.8	0.735	0.914
$GSr_E/TpSr_E$, ms^{-2} *100	1.8 ± 1.1	1.5 ± 0.9	1.3 ± 0.6	0.099	0.173

Global peak systolic strain rate (GSr) and the acceleration of systolic deformation (GSr/TpSr) were significantly reduced with increased severity of angiographic lesions. Time to peak systolic strain rate (TpSr) was significantly longer in group 2 than in group 1, but not significantly different between group 2 and 3. Global diastolic Sr parameters (GSr_E, GSr_A) were found to differ significantly between group 1 and 2.

In all 3 longitudinal views, global peak systolic strain rate (GSr) was significantly reduced with increased severity of angiographic lesions. Time to peak systolic strain rate (TpSr) was significantly longer in group 2 than in group 1, but did not differ significantly between group 2 and 3.

The diastolic strain rate parameters (GSr_E, GSr_A) differed significantlyt between 2 and 3. The comparison of the ratio of early and late diastolic global strain rate between the patient groups showed no significant difference in all 3 longitudinal views (table 15- 17).

The ratio of time to peak systolic and diastolic strain rate ($TpSr/TpSr_E$) was significantly higher in group 2 than in group 1, but with no significant differences between group 2 and 3 in longitudinal and SAX views (table 13-17).

Table 15. Longitudinal Sr and derived parameters in 4CH

	Group 1 (n=56)	Group 2 (n=87)	Group 3 (n=59)	P value	
				1:2	2:3
GSr , s^{-1}	-1.3 ± 0.2	-1.1 ± 0.2	-0.9 ± 0.2	0.000	0.000
TpSr, ms	118.0 ± 17.3	162.4 ± 34.2	163.9 ± 31.7	0.000	0.787
GSr/TpSr, ms^{-2} *100	-1.1 ± 0.2	-0.7 ± 0.2	-0.5 ± 0.1	0.000	0.000
GSr_E, s^{-1}	1.8 ± 0.4	1.6 ± 0.4	1.3 ± 0.4	0.004	0.000
GSr_A, s^{-1}	0.5± 0.2	0.5± 0.2	0.4± 0.2	0.090	0.008
GSr_E/GSr_A	4.3 ± 3.2	5.3 ± 4.9	6.5 ± 9.7	0.162	0.365
$TpSr_E$, ms	129.7 ± 22.7	132.4 ± 35.7	134.1 ± 31.4	0.583	0.761
$GSr_E/TpSr_E$, ms^{-2} *100	1.4 ± 0.5	1,4 ± 0.9	1.0 ± 0.4	0.438	0.001

Table 16. Longitudinal Sr and derived parameters in APLAX

	Group 1 (n=56)	Group 2 (n=86)	Group 3 (n=57)	P value	
				1:2	2:3
GSr, s^{-1}	-1.3 ± 0.2	-1.1 ± 0.3	-1.0 ± 0.2	0.000	0.004
TpSr, ms	118.9 ± 15.0	169.2 ± 38.6	159.4 ± 35.1	0.000	0.118
GSr/TpSr, ms^{-2} *100	-1.1 ± 0.2	-0.7 ± 0.2	-0.6 ± 0.2	0.000	0.162
GSr_E, s^{-1}	1.8 ± 0.5	1.6 ± 0.5	1.3 ± 0.4	0.032	0.000
GSr_A, s^{-1}	0.5 ± 0.3	0.5 ± 0.2	0.4 ± 0.2	0.132	0.012
GSr_E/GSr_A	4.2 ± 3.0	5.0 ± 5.4	5.7 ± 5.3	0.236	0.445
$TpSr_E$, ms	130.7 ± 21.1	139.4 ± 33.3	134.6 ± 28.8	0.059	0.363
$GSr_E/TpSr_E$, ms^{-2} *100	1.4 ± 0.5	1.2 ± 0.5	1.0 ± 0.4	0.049	0.012

Table 17. Longitudinal Sr and derived parameters in 2CH

	Group 1 (n=46)	Group 2 (n=33)	Group 3 (n=40)	P value	
				1:2	2:3
GSr, s^{-1}	-1.3 ± 0.2	-1.1 ± 0.2	-1.0 ± 0.2	0.003	0.003
TpSr, ms	115.9 ± 16.0	168.6 ± 30.9	155.6 ± 27.7	0.000	0.067
GSr/TpSr, ms^{-2} *100	-1.1 ± 0.2	-0.7 ± 0.2	-0.6 ± 0.2	0.000	0.294
GSr_E, s^{-1}	1.5 ± 0.4	1.4 ± 0.4	1.2 ± 0.4	0.185	0.006
GSr_A, s^{-1}	0.6 ± 0.3	0.6 ± 0.3	0.4 ± 0.2	0.668	0.007
GSr_E/GSr_A	3.2 ± 1.6	3.3 ± 2.1	3.9 ± 3.2	0.734	0.321
$TpSr_E$, ms	131.6 ± 22.6	137.6 ± 26.2	128.7 ± 32.5	0.286	0.199
$GSr_E/TpSr_E$, ms^{-2} *100	1.2± 0.4	1.1± 0.4	1.0 ± 0.4	0.207	0.251

We compared the longitudinal systolic strain rate parameters in each longitudinal view to each other within each group. No significant differences in the longitudinal strain rate parameters, except in global peak systolic strain rate (GSr) and acceleration of systolic deformation (GSr/TpSr) in group 3, were found within each group (table 18).

Table 18. Longitudinal Sr and derived parameters in each group

	4CH	APLAX	2CH	P value		
				4CH:APLAX	4CH:2CH	APLAX:2CH
Group 1						
GSr , s^{-1}	-1.3 ± 0.2	-1.3 ± 0.2	-1.3 ± 0.2	0.568	0.153	0.065
TpSr, ms	118.0 ± 17.3	118.9 ± 15.0	115.9 ± 16.0	0.753	0.535	0.332
GSr/TpSr, ms^{-2} *100	-1.1 ± 0.2	-1.1 ± 0.2	-1.1 ± 0.2	0.813	0.374	0.291
Group 2						
GSr , s^{-1}	-1.1 ± 0.2	-1.1 ± 0.3	-1.1 ± 0.2	0.788	0.776	0.986
TpSr, ms	162.4 ± 34.2	169.2 ± 38.6	168.6 ± 30.9	0.225	0.352	0.924
GSr/TpSr, ms^{-2} *100	-0.7 ± 0.2	-0.7 ± 0.2	-0.7 ± 0.2	0.675	0.679	0.960
Group 3						
GSr , s^{-1}	-0.9 ± 0.2	-1.0 ± 0.2	-1.0 ± 0.2	0.005	0.035	0.687
TpSr, ms	163.9 ± 31.7	159.4 ± 35.1	155.6 ± 27.7	0.464	0.170	0.557
GSr/TpSr, ms^{-2} *100	-0.5 ± 0.1	-0.6 ± 0.2	-0.6 ± 0.2	0.003	0.013	0.998

3.3.2.2.3. Synchrony parameters

All the studied synchrony parameters were significantly higher with increased severity of angiographic lesions in SAX and longitudinal views (table 19, 20), showing an increasing degree of asynchrony.

Table 19. Strain-derived synchrony parameters in SAX

	Group 1 (n=45)	Group 2 (n=69)	Group 3 (n=42)	P value	
				1:2	2:3
Radial					
$TpS_{disp.}$, ms	27.6 ± 22.5	47.2 ± 34.8	67.7 ± 50.8	0.000	0.024
SD_{TpS}, ms	13.1 ± 10.9	22.3 ± 16.8	32.8 ± 24.6	0.001	0.017
$Index_{asynch.}$	4.2 ± 3.5	6.3 ± 4.9	8.8 ± 6.7	0.009	0.034
Circumferential					
$TpS_{disp.}$, ms	48.1 ± 34.4	84.9 ± 30.6	123.4 ± 45.8	0.000	0.000
SD_{TpS}, ms	22.9 ± 18.1	40.2 ± 15.5	51.6 ± 17.1	0.000	0.001
$Index_{asynch.}$	7.3 ± 5.6	11.7 ± 4.4	15.1 ± 5.1	0.000	0.001

Table 20. Strain-derived synchrony parameters in apical views

	Group 1	Group 2	Group 3	P value	
				1:2	2:3
4 CH	n=56	n=87	n=59		
$TpS_{disp.}$, ms	46.5 ± 23.3	79.7 ± 21.1	131.6 ± 37.0	0.000	0.000
SD_{TpS}, ms	22.2 ± 13.7	35.6 ± 12.3	56.9 ± 17.0	0.000	0.000
$Index_{asynch.}$	7.2 ± 4.0	10.2 ± 3.3	16.0 ± 4.9	0.000	0.000
APLAX	n=56	n=86	n=57		
$TpS_{disp.}$, ms	42.8 ± 23.5	80.9 ± 22.7	125.6 ± 34.0	0.000	0.000
SD_{TpS}, ms	20.2 ± 11.5	37.6 ± 13.0	57.0 ± 16.3	0.000	0.000
$Index_{asynch.}$	6.8 ± 3.7	10.9 ± 3.7	16.3 ± 5.4	0.000	0.000
2 CH	n=46	n=33	n=40		
$TpS_{disp.}$, ms	54.6 ± 25.4	81.9 ± 15.4	123.7 ± 27.4	0.000	0.000
SD_{TpS}, ms	25.5 ± 12.9	36.5 ± 8.9	52.6 ± 11.5	0.000	0.000
$Index_{asynch.}$	8.0 ± 3.8	10.3 ± 2.3	14.8 ± 3.3	0.001	0.000

We compared the longitudinal strain-derived synchrony parameters in each longitudinal view to each other within each group. No significant differences in the longitudinal strain synchrony parameters, except in dispersion of time to peak systolic strain ($TpS_{disp.}$) and one standard deviation of the time to peak systolic strain (SD_{TpS}) in group 1, was found within each group (table 21).

Table 21. Longitudinal strain-derived synchrony parameters in each group

	4 CH	APLAX	2 CH	P value		
				4CH:APLAX	4CH:2CH	APLAX:2CH
Group 1						
$TpS_{disp.}$, ms	46.5 ± 23.3	42.8 ± 23.5	54.6 ± 25.4	0.409	0.101	0.018
SD_{TpS}, ms	22.2 ± 13.7	20.2 ± 11.5	25.5 ± 12.9	0.410	0.214	0.033
$Index_{asynch.}$	7.2 ± 4.0	6.8 ± 3.7	8.0 ± 3.8	0.505	0.356	0.109
Group 2						
$TpS_{disp.}$, ms	79.7 ± 21.1	80.9 ± 22.7	81.9 ± 15.4	0.713	0.525	0.781
SD_{TpS} , ms	35.6 ± 12.3	37.6 ± 13.0	36.5 ± 8.9	0.309	0.665	0.612
$Index_{asynch.}$	10.2 ± 3.3	10.9 ± 3.7	10.3 ± 2.3	0.198	0.911	0.277
Group 3						
$TpS_{disp.}$, ms	131.6 ± 37.0	125.6 ± 34.0	123.7 ± 27.4	0.371	0.229	0.758
SD_{TpS}, ms	56.9 ± 17.0	57.0 ± 16.3	52.6 ± 11.5	0.979	0.139	0.126
$Index_{asynch.}$	16.0 ± 4.9	16.3 ± 5.4	14.8 ± 3.3	0.717	0.168	0.094

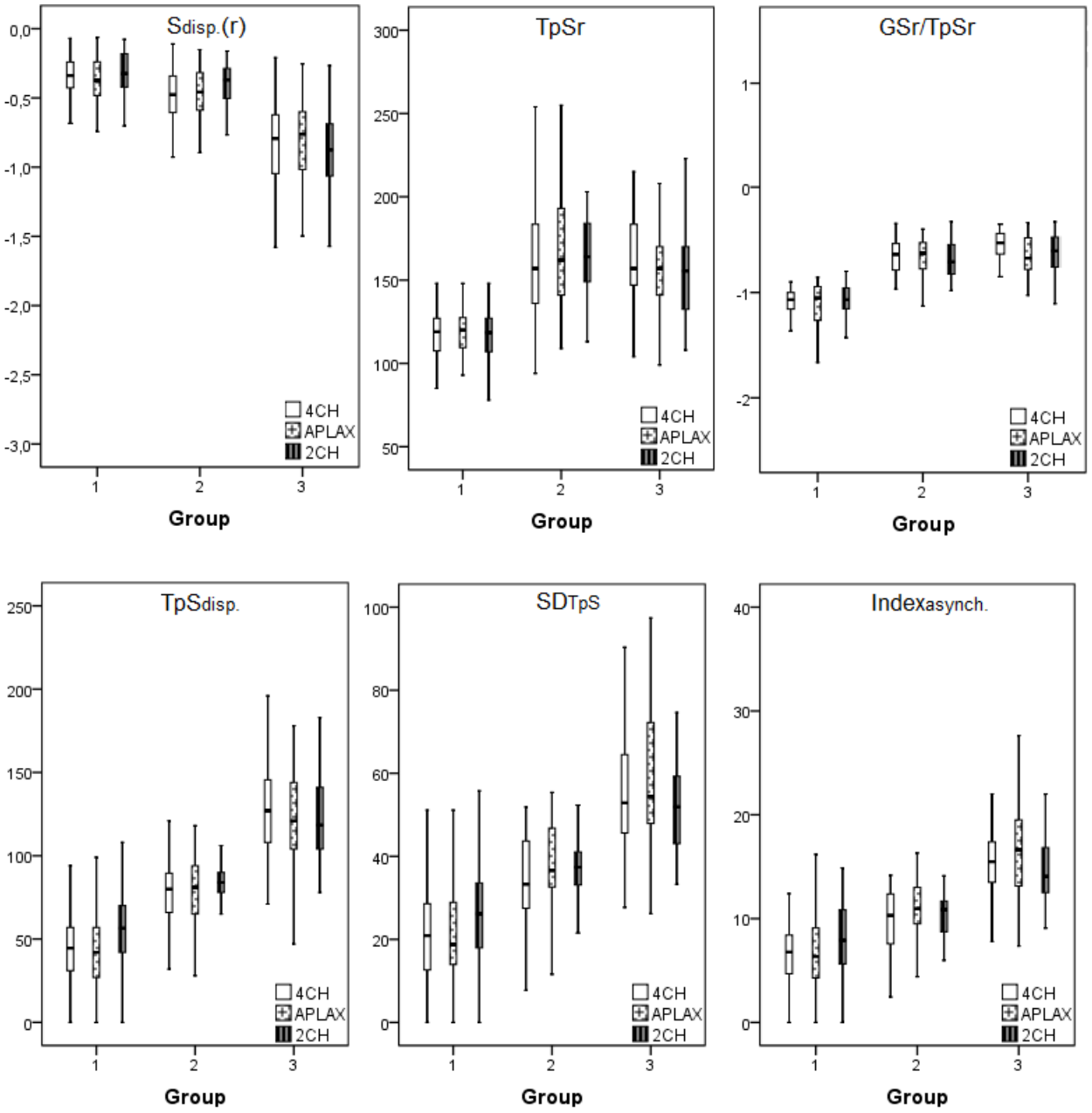

Figure 6. Selected systolic strain, strain rate and synchrony parameters obtained from 3 longitudinal views in the 3 patient groups.

Time to peak longitudinal systolic strain (TpSr) and the acceleration of longitudinal systolic deformation (GSr/TpSr) showed a significant difference between group 1 and 2, but no significant difference between group 2 and 3. Relative dispersion of global longitudinal systolic strain ($S_{disp.}(r)$) significantly increased in group 3 compared with group 1 and 2. All the three strain-derived synchrony parameters showed a significant increase with increased angiographic severity.
The above parameters of each longitudinal view showed no significant difference in each group.

3.3.2.5. Predictability of speckle tracking echocardiography for the prediction of CAV

We selected the strain, Sr, and derived parameters, that differed significantly between the three groups, and used the ROC to determine their diagnostic values for CAV.

3.3.2.5.1. The ROC analysis of strain, Sr, and derived parameters

The ROC analysis of STE parameters in SAX view showed that time to peak circumferential systolic strain rate (TpSrC) and circumferential acceleration of systolic deformation (GSrC/TpSrC) had relatively high diagnostic values for CAV with no focal stenosis (table 24).

Table 22. The ROC analysis of radial strain, Sr, and derived parameters for prediction of CAV with no focal stenosis (Group 1:2)

	AUC(%)	95% CI	Cut-off	Sensitivity(%)	Specificity(%)
$S_{disp.}$	64.2	0.54-0.74	≥ 11.7	60.9	60
$S_{disp.}(r)$	63.3	0.53-0.73	≥26.7, but <41.1	62.3	62.2
TpSr	83.8	0.76-0.91	≥137.5	73.9	77.8
GSr/TpSr	73.3	0.64-0.82	≤1.4, but >1.1	65.2	66.7
$TpSr/TpSr_E$	66.5	0.56-0.76	≥1.1	65.2	37.8

Table 23. The ROC analysis of radial strain, Sr, and derived parameters for prediction of CAV with focal stenosis (Group 2:3)

	AUC(%)	95% CI	Cut-off	Sensitivity(%)	Specificity(%)
GS	72.9	0.63-0.83	≤37.4	76.2	60.9
$S_{disp.}(r)$	65.8	0.55-0.76	≥41.1	61.9	62.3
GSr	66.6	0.56-0.77	≤1.8	66.7	60.9
GSr/TpSr	65.4	0.55-0.76	≤1.1	61.9	63.8

Table 24. The ROC analysis of circumferential strain, Sr, and derived parameters for prediction of CAV with no focal stenosis (Group 1:2)

	AUC(%)	95% CI	Cut-off	Sensitivity(%)	Specificity(%)
GS	75.0	0.66-0.84	≥-19.1	69.6	68.9
$S_{disp.}(r)$	69.4	0.60-0.79	≥73.7, but<99.2	63.8	66.7
GSr	75.9	0.67-0.85	≥-1.4	71.0	66.7
TpSr	88.7	0.82-0.95	≥136	81.2	86.7
GSr/TpSr	90.1	0.85-0.96	≥-1.0, but<-0.7	81.2	80.0
$TpSr/TpSr_E$	70.5	0.61-0.80	≥1.1	63.8	68.9

Table 25. The ROC analysis of circumferential strain, Sr, and derived parameters for prediction of CAV with focal stenosis (Group 2:3)

	AUC(%)	95% CI	Cut-off	Sensitivity(%)	Specificity(%)
GS	71.1	0.61-0.81	≥-16.1, but<-19.1	76.2	65.2
$S_{disp.}(r)$	68.0	0.58-0.78	≥99.2	66.7	62.3
GSr	71.6	0.62-0.81	≥-1.1	61.9	60.9
GSr/TpSr	68.1	0.58-0.78	≥-0.7	66.7	60.9

The ROC analysis of longitudinal STE parameters in 4CH, APLAX, and 2CH showed that time to peak systolic strain rate (TpSr) and acceleration of systolic deformation (GSr/TpSr) had high diagnostic values for CAV with no focal stenoses (table 26,28,30) and peak systolic strain relative dispersion ($S_{dis.}(r)$) had relatively high diagnostic values for CAV with focal stenoses (table 27, 31).

Table 26. The ROC analysis of longitudinal strain, Sr, and derived parameters in 4CH for prediction of CAV with no focal stenosis (Group 1:2)

	AUC(%)	95% CI	Cut-off	Sensitivity(%)	Specificity(%)
GSr	76.8	0.69-0.84	≥-1.2,but<-1.0	66.7	80.4
TpSr	90.4	0.85-0.95	≥129.0	87.4	82.1
GSr/TpSr	98.5	0.97-1	≥-0.9	93.1	94.6
$TpSr/TpSr_E$	80.3	0.73-0.87	≥1	70.1	75.0

Table 27. The ROC analysis of longitudinal strain, Sr, and derived parameters in 4CH for prediction of CAV with focal stenosis (Group 2:3)

	AUC(%)	95% CI	Cut-off	Sensitivity(%)	Specificity(%)
GS	80.9	0.74-0.88	≥-15.9	71.2	71.3
$S_{disp.}$	68.4	0.60-0.77	≥9.8	62.7	69.0
$S_{disp.}(r)$	82.4	0.75-0.89	≤-59.0	81.4	74.7
GSr	78.4	0.71-0.86	≥-1.0	72.9	67.8
GSr_E	72.3	0.64-0.81	≤1.4	64.4	66.7

Table 28. The ROC analysis of longitudinal strain, Sr, and derived parameters in APLAX for prediction of CAV with no focal stenosis (Group 1:2)

	AUC(%)	95% CI	Cut-off	Sensitivity(%)	Specificity(%)
GSr	74.3	0.66-0.82	≥-1.2,but<1.0	64.0	67.9
TpSr	91.5	0.87-0.96	≥129.0	84.9	80.4
GSr/TpSr	94.7	0.91-0.98	≥-0.9	89.5	91.1
TpSr/$TpSr_E$	79.6	0.72-0.87	≥1	65.1	78.6

Table 29. The ROC analysis of longitudinal strain, Sr, and derived parameters in APLAX for prediction of CAV with focal stenosis (Group 2:3)

	AUC(%)	95% CI	Cut-off	Sensitivity(%)	Specificity(%)
GS	73.8	0.65-0.82	≥-15.9	61.4	70.9
$S_{disp.}$	70.5	0.62-0.79	≥9.8	64.9	66.3
$S_{disp.}$(r)	83.1	0.76-0.90	≤-58.0	77.2	74.4
GSr	66.8	0.58-0.76	≥-1.0	56.1	68.6
GSr_E	67.6	0.58-0.77	≤1.4	61.4	64.0

Table 30. The ROC analysis of longitudinal strain, Sr, and derived parameters in 2CH for prediction of CAV with no focal stenosis (Group 1:2)

	AUC(%)	95% CI	Cut-off	Sensitivity(%)	Specificity(%)
GSr	69.0	0.57-0.81	≥-1.2,but<1.0	66.7	69.6
TpSr	95.9	0.91-1	≥129.0	93.9	84.8
GSr/TpSr	97.2	0.94-1	≥-0.9	90.9	93.5
TpSr/$TpSr_E$	85.4	0.77-0.94	≥1	72.7	80.4

Table 31. The ROC analysis of longitudinal strain, Sr, and derived parameters in 2CH for prediction of CAV with focal stenosis (Group 2:3)

	AUC(%)	95% CI	Cut-off	Sensitivity(%)	Specificity(%)
GS	78.8	0.69-0.89	≥-16.1	65.0	72.7
$S_{disp.}$	79.8	0.70-0.90	≥9.8	62.5	75.8
$S_{disp.}$(r)	90.4	0.84-0.97	≤-60.2	80.0	87.9
GSr	68.0	0.56-0.80	≥-1	65.0	60.6
GSr_E	67.3	0.55-0.80	≤1.3	67.5	60.6

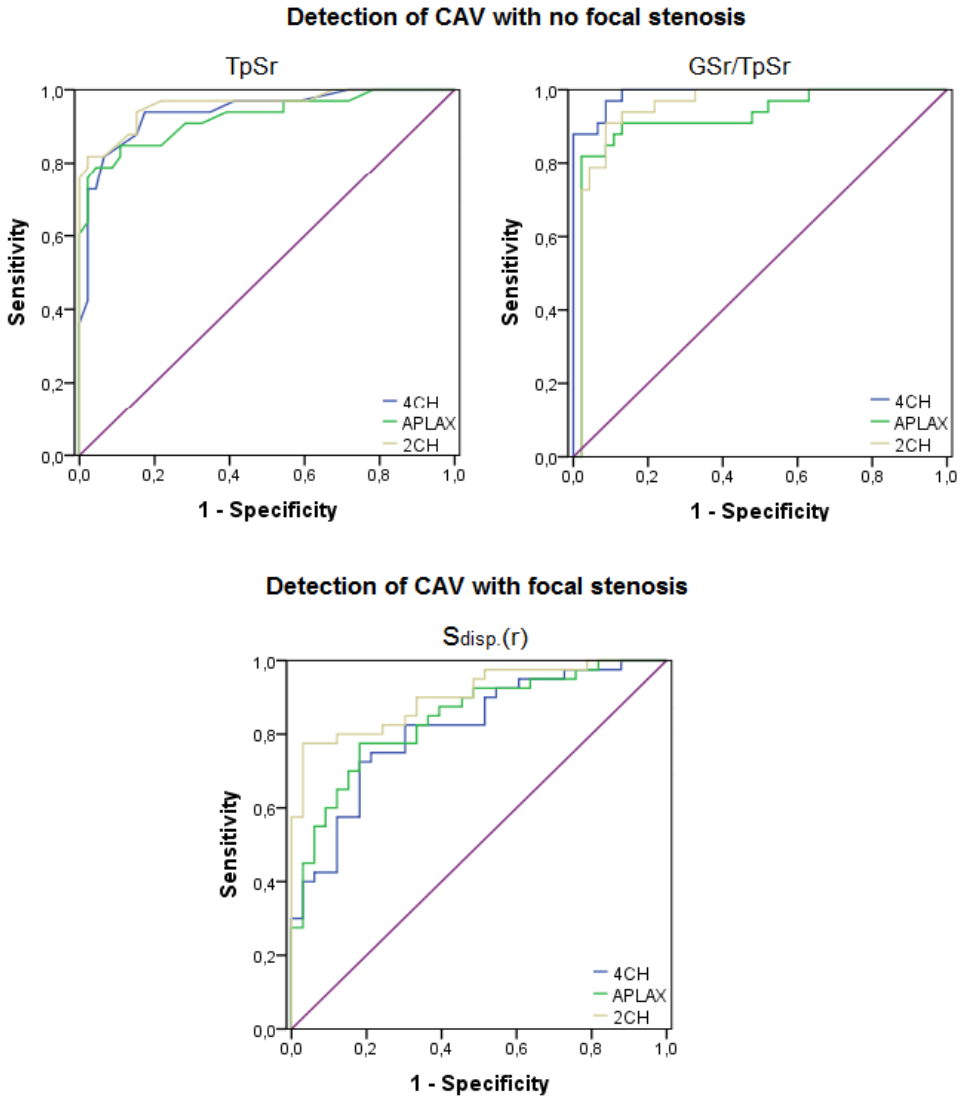

Figure 7. ROC curves of longitudinal strain and strain rate parameters for detection of CAV.

Time to peak longitudinal systolic strain rate (TpSr) and the longitudinal acceleration of systolic deformation (GSr/TpSr) showed high diagnostic values for CAV with no focal stenoses.
Peak longitudinal strain relative dispersion ($S_{disp.}(r)$) showed relative high diagnostic values for CAV with focal stenoses.
The parameters of each longitudinal view showed similar diagnostic values for CAV.

3.3.2.5.2. The ROC analysis of strain-derived synchrony parameters

The ROC analysis showed relatively low diagnostic values of parasternal short axis strain-derived parameters for prediction of CAV (table 32).

Table 32. The ROC analysis of strain-derived synchrony parameters in SAX

	CAV with no focal stenosis (Group 1:2)					CAV with focal stenosis (Group 2:3)				
	AUC (%)	95% CI	Cut-off	Sensi. (%)	Speci. (%)	AUC (%)	95% CI	Cut-off	Sensi. (%)	Speci. (%)
Radial										
$TpS_{disp.}$	68.7	0.59-0.79	≥28.5,but <67.5	55.9	62.2	59.7	0.48-0.71	≥67.5	50.0	66.2
SD_{TpS}	67.5	0.57-0.77	≥14.5,but <24.4	55.9	60.0	60.6	0.49-0.72	≥24.4	57.1	61.9
$Index_{asynch.}$	62.4	0.52-0.73	≥5.0, but <6.8	50.0	60.0	59.9	0.48-0.71	≥6.8	54.8	60.3
Circumferential										
$TpS_{disp.}$	82.1	0.74-0.90	≥61.0,but <102.5	79.4	79.3	74.8	0.65-0.84	≥102.5	64.3	73.5
SD_{TpS}	79.7	0.71-0.88	≥31.2,but <45.4	72.1	75.0	69.2	0.59-0.79	≥45.4	66.7	32.4
$Index_{asynch.}$	76.9	0.67-0.86	≥9.6, but <13.1	73.5	75.0	69.1	0.59-0.79	≥13.1	64.3	63.2

Table 33. The ROC analysis of strain-derived synchrony parameters in apical views

	CAV with no focal stenosis(Group 1:2)					CAV with focal stenosis(Group 2:3)				
	AUC (%)	95% CI	Cut-off	Sensi. (%)	Speci. (%)	AUC (%)	95% CI	Cut-off	Sensi. (%)	Speci. (%)
4CH										
$TpS_{disp.}$	86.3	0.80-0.93	≥62.5,but <100.5	81.4	80.4	90.8	0.86-0.96	≥100.5	84.7	84.9
SD_{TpS}	80.0	0.72-0.88	≥27.5,but <44.8	76.7	71.4	86.2	0.80-0.92	≥44.8	79.7	80.2
$Index_{asynch.}$	74.2	0.65-0.83	≥8.5, but <12.7	70.9	75.0	85.9	0.80-0.92	≥12.7	81.4	81.4
APLAX										
$TpS_{disp.}$	87.5	0.82-0.93	≥62.5,but <101.5	83.5	78.6	88.1	0.82-0.94	≥101.5	80.7	83.5
SD_{TpS}	84.8	0.78-0.91	≥27.6,but <44.6	81.2	75.0	83.6	0.77-0.90	≥44.6	78.9	74.1
$Index_{asynch.}$	79.9	0.72-0.88	≥8.4, but <12.8	77.6	71.4	81.8	0.75-0.89	≥12.8	75.4	74.1
2CH										
$TpS_{disp.}$	83.3	0.74-0.93	≥72.5,but <98.5	84.4	80.4	93.7	0.88-0.99	≥98.5	85.0	87.5
SD_{TpS}	76.7	0.66-0.87	≥32.5,but <41.2	78.1	73.9	88.1	0.80-0.96	≥41.2	82.5	78.1
$Index_{asynch.}$	69.9	0.58-0.82	≥10.4,but <12.2	65.6	69.6	89.8	0.83-0.97	≥12.2	85.0	87.5

The ROC analysis showed relatively high diagnostic values of longitudinal apical axis strain-derived parameters for prediction of CAV.

Dispersion of time to peak systolic strain ($TpS_{disp.}$) showed high diagnostic values for CAV with and without focal stenoses. $Index_{aynch.}$ showed also high diagnostic values for CAV in four and two chamber views.

Each parameter of each longitudinal view showed similar diagnostic values for CAV.

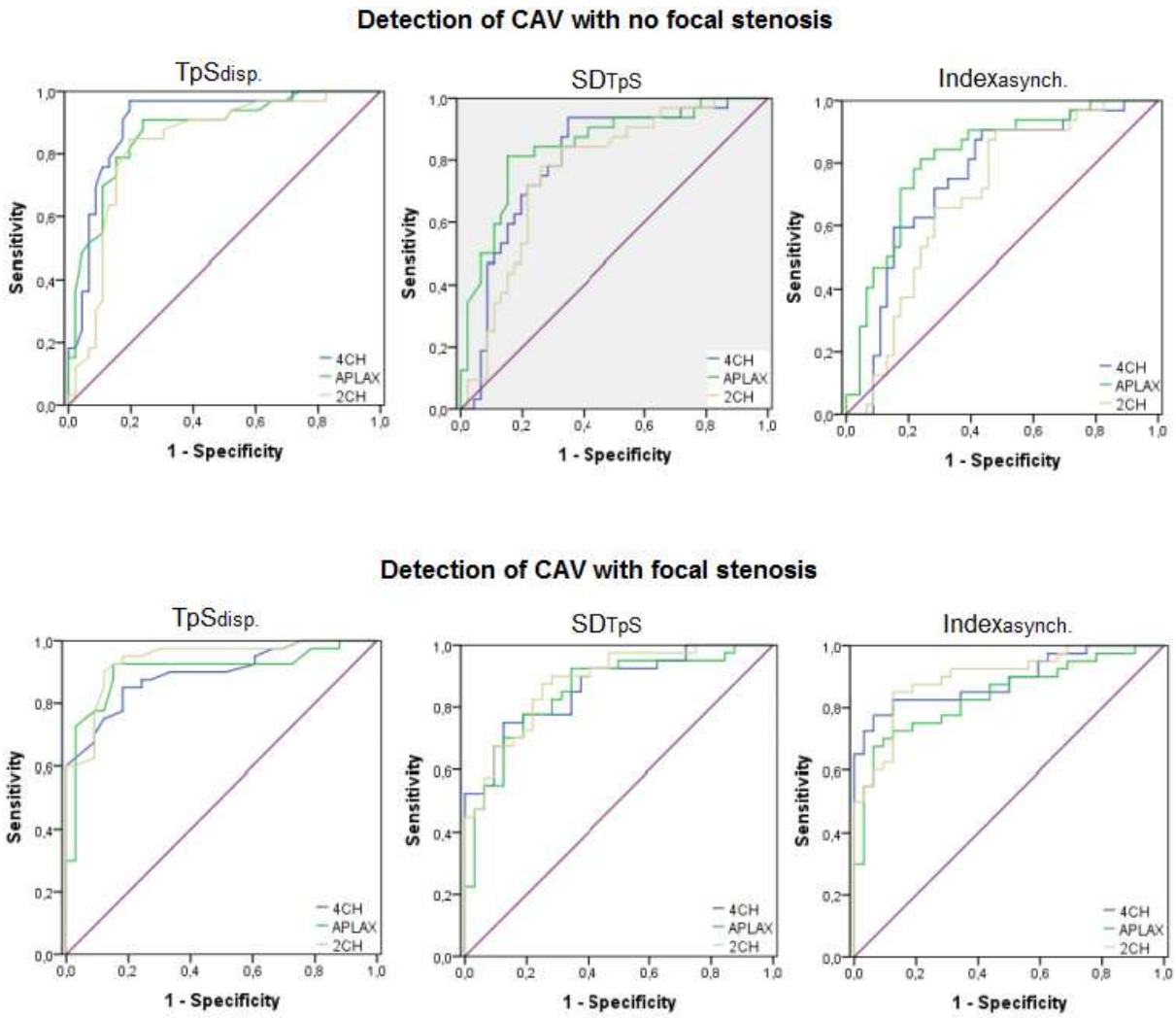

Figure 8. ROC curves of longitudinal strain-derived synchrony parameters for detection of CAV.

Dispersion of time to peak longitudinal systolic strain ($TpS_{disp.}$) showed relative high diagnostic values for CAV with and without focal stenoses in all longitudinal views. $Index_{asynch.}$ in 4 and 2CH views showed also relative high diagnostic values for CAV with focal stenoses.
Each synchrony parameter of each longitudinal view showed similar diagnostic values for CAV.

3.3.2.5.3. Predictive value of STE for CAV

Most of the STE parameters, that appeared to be significantly diagnostic for CAV, were not significantly different in 4CH, APLAX, and 2CH in each of the three groups (Table 12, 18, 21). The ROC analyses showed similar sensitivities and specificities of these parameters in 4CH, APLAX, and 2CH (Table 26-31,33), for prediction of CAV, and longitudinal STE parameters showed higher diagnostic values than in SAX (table 22-25). The 4CH view (see the discussion section) was easier to record and gave images of better quality than APLAX and 2CH.
Hence, we selected the STE parameters in 4CH to assess the predictive values of STE for CAV.

Time to peak longitudinal systolic strain rate (TpSrL) and the longitudinal acceleration of systolic deformation (GSrL/TpSrL) showed the highest predictive values for CAV with no focal stenosis (table 34).

The peak longitudinal systolic strain relative dispersion ($SL_{disp.}(r)$.), the dispersion of time to peak longitudinal systolic strain ($TpSL_{disp.}$), and the intraventricular asynchrony index ($index_{asynch.}$) showed high negative predictive values for CAV with focal stenosis (table 35).

Table 34. Predictive values of STE for the prediction of CAV with no focal stenosis

	Cut-off	PPV(%)	NPV(%)
TpSrL	≥129.0	88.4	80.7
GSrL/TpSrL	≥-0.9	96.4	89.8
$TpSL_{disp.}$	≥62.5, but<100.5	73.8	84.3

Table 35. Predictive value of STE for the prediction of CAV with focal stenosis

	Cut-off	PPV(%)	NPV(%)
$SL_{disp.}(r)$	≤-59.9	69.0	86.7
$TpSL_{disp.}$	≥100.5	79.4	89.2
$Index_{asynchr.}$	≥12.7	76.2	86.7

On the basis of the diagnostic values of STE parameters, we developed a flow-chart of the prediction of CAV; it includes acceleration of longitudinal systolic deformation, longitudinal dyssynchrony and dyssynergy parameters (Figure 9).

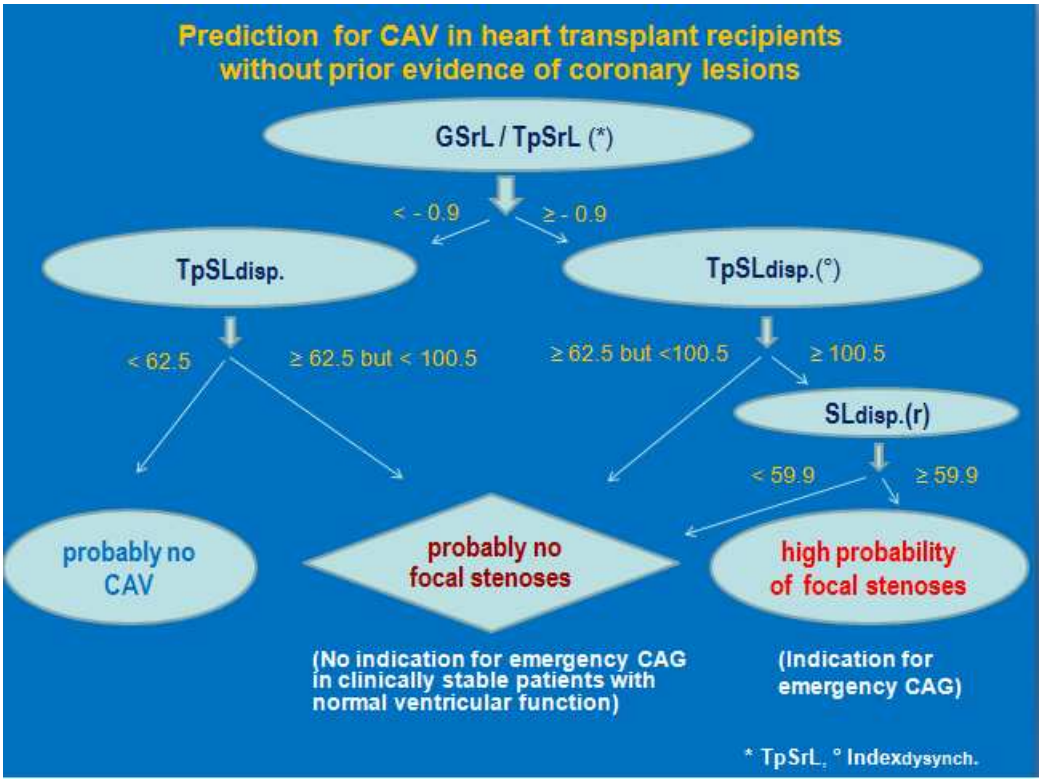

Figure 9. The STE-based flow-chart of prediction for CAV

Longitudinal acceleration of systolic deformation (GSrL/TpSrL) can differentiate at a cutoff of -0.9 between heart transplant recipients with normal angiogram and CAV with no focal stenoses with very high positive and negative predictive values. Dispersion of time to peak longitudinal systolic strain ($TpSL_{disp.}$) <62.5 can exclude CAV with no focal stenoses with a high negative predictive value.
Definite cutoff values for $TpSL_{disp.}$ and peak longitudinal systolic strain relative dispersion ($SL_{disp.}(r)$.) can distinguish between CAV with and without focal stenoses with relative high negative predictive values.
Time to peak longitudinal systolic strain rate (TpSrL) and $Index_{asynch.}$ can be substituted for GSrL/TpSrL, and $TpSL_{disp.}$, respectively, with high predictive values.

3.4. Discussion

The lack of early clinical symptoms due to graft denervation makes the diagnosis of CAV difficult in heart transplant recipients. Furthermore, unlike native atherosclerotic coronary artery disease, which is usually characterized by focal and eccentric stenosis of epicardial coronary vessels, CAV is characterized by diffuse and rapidly progressive intimal thickening in the entire coronary arteries, later leading to luminal narrowing and occlusion of small arteries. This means that CAV can be under-diagnosed on one-time coronary angiography, stressing that angiograms should be interpreted serially.

The routine annual performance of coronary angiography for CAV screening, however, has the risks associated with the invasive method and also a high risk of renal failure in heart transplant recipients. Efforts to determine the optimal timing of coronary angiography by using noninvasive methods, which are reliable and repeatable, are advocated by some studies.[5,57]

Echocardiographic strain reveals alterations in wall motion and myocardial deformation, which is not detectable by conventional echocardiography, and allows distinction between active and passive wall motion.[87]

The aim of our study was to assess the reliability of speckle-tracking echocardiography (STE), which has been recently developed, in distinguishing patients with and without angiographic CAV after heart transplantation.

3.4.1. Diagnostic value of STE for CAV

Our study showed that conventional echocardiography is insensitive and unspecifitic in the prediction of CAV in transplant recipients who have normal left ventricular systolic function. Left ventricular end-diastolic diameter was significantly increased in CAV patients with no focal stenosis compared to the patients with normal angiogram (4.8±0.4cm vs. 4.6±0.5cm), and wall thicknesses were significantly increased in CAV patients with focal stenosis compared to patients with normal angiogram and with no focal stenosis. Left ventricular systolic function, defined as LVEF and LVFS, appeared to be significantly reduced in group 3 than in group 1 and 2, but remained within the normal range. These results were in agreement with those of Wilhelmi et al[37] that, more than 10 years after transplantation, cardiac grafts were characterized by normal left ventricular dimensions and ejection fraction with left ventricular hypertrophy. As in the

study by St Goar et al,[38] the restrictive pattern (E/A >2, shorter deceleration time of E wave, and shorter isovolumetric relaxation time) was found in our groups and appeared to be worsened with increased severity of angiographic lesions. However, the conventional echocardiographic parameters had a low sensitivity and a low specificity of 52 to 65.9% and 56.3 to 61.8%, respectively, for prediction of angiographic CAV.

There are few studies that address the usefulness of strain and strain rate imaging in the prediction of CAV after heart transplantation. To assess the reliabilaty of strain and strain rate imaging in predicting CAV, we analyzed 12 systolic and diastolic STE-derived parameters in parasternal short and apical long axis views.

First, our results showed that systolic strain and strain rate parameters are capable of distinguishing the patients with angiographic CAV.

Global peak systolic strain values were significantly lower in CAV patients without focal stenoses than in heart transplant recipients with normal angiograms in circumferential, apical 4-chamber, and apical long axis strain imagings, respectively. In all views studied, global peak systolic strain values showed a significant reduction in CAV patients with focal stenosis compared with CAV patients without focal stenoses.

Peak systolic strain relative dispersion increased significantly with increased severity of angiographic lesions in all the views studied.

Global peak systolic strain rate (GSr) showed also a significant reduction in CAV patients without focal stenoses compared with the heart transplant recipients with normal angiograms in the circumferential and all three longitudinal stain imagings. In all views studied, global peak systolic strain rate values showed significant reduction in CAV patients with focal stenosis compared with CAV patients without focal stenoses.

Global peak systolic strain rate was significantly delayed, reflected as an increase in time to peak systolic strain rate (TpSr), in patients with angiographic CAV with no focal stenosis in comparison with the heart transplant recipients with normal angiograms, but TpSr showed no difference between CAV groups with and without focal stenosis in all the views. The combination of GSr and TpSr, (acceleration of systolic strain) showed a highly significant reduction with increased severity of angiographic lesions in all the views studied.

All the strain-derived synchrony parameters, including dispersion of time to peak systolic strain ($TpS_{disp.}$), one standard deviation of the time to peak systolic strain (SD_{TpS}), and intraventricular asynchrony index ($Index_{aynch.}$), showed a significant increase in CAV patients without focal

stenoses compared with the heart transplant recipients with normal angiograms, and in CAV patients with focal stenosis compared to CAV patients without focal stenoses.

Among the strain and strain rate parameters, that differed between the groups, we found that TpSr and the acceleration of circumferential and longitudinal systolic deformation had the highest values in prediction of diffuse CAV without focal stenosis. $S_{disp.}(r)$ showed a relatively high diagnostic value for CAV with focal stenosis. In three longitudinal views, $TpS_{disp.}$ and $Index_{asynch.}$ showed high diagnostic values in distinguishing the patients with increased severity of angiographic lesions.

The parameters, that reflect the extent of strain and strain rate, showed a significant reduction in angiographic CAV patients with no focal stenosis compared to angiographically normal patients in all the views, except for the radial view, but the difference was not great enough to distinguish the two groups with high diagnostic strength. In contrast, the parameters which reflect the timing of strain and strain rate (strain-derived synchrony parameters and TpSr) showed highly significant differences between the heart transplant recipients with normal angiograms and the patients with CAV with no focal stenosis, so that these parameters had very high diagnostic values for CAV with no focal stenosis. TpSr was no longer increased in CAV patients with focal stenosis in comparison to patients without focal stenosis in all the views, but the strain dispersion rose from group 1 to group 2 and again to group 3. These results suggest that the angiographic changes in coronary arteries after heart transplantation might be expressed first of all by the changes in the timing of strain and strain rate, and be followed, with development of angiographic severity, by changes in its extent on speckle-tracking echocardiograms.

Because the final part of ejection occurs by inertial effects after myocyte contraction is finished, peak systolic global strain rate, being an early systolic event, is more closely related to contractility than the EF, and impaired systolic function can be detected earlier by peak systolic strain rate than by EF measurements.[87]

Second, our results showed that longitudinal strain imaging may be superior to parasternal short axial strain imaging in prediction of angiographic CAV.

ROC analysis showed relative low sensitivities and specificities of the radial and circumferential strain and strain rate parameters, except for TpSr and the GSr/TpSr in circumferential strain imaging, compared with those of the longitudinal strain and strain rate parameters in predicting CAV with and without focal stenosis. These differences of diagnostic performance in short axial and longitudinal strain and strain rate may be attributed to several factors: because longitudinal course predominates in the subendocardium, which is more susceptible to myocardial ischemia

than the subepicardium,[51] longitudinal strain and strain rate imaging is more suitable to assess the myocardial ischemia in the subendocardium than the strain and strain imaging in short axis views. As the image quality with transthoracic echocardiography is frequently suboptimal after heart surgery and the heart location is changed after heart transplantation, it was not easier to obtain images of good quality in parasternal short axis view than in longitudinal apical views in heart transplant recipients. We obtained the parasternal short axis images of good quality for the evaluation of speckle tracking imaging in 156 patients (77%) and failed to analyze the radial and circumferential strain and strain rate in 23% patients because of poor image quality. In contrast, all the patients had good image quality with apical four chamber imaging.

Third, our results showed that the STE parameters in apical 4 chamber view are capable to detect CAV with high diagnostic values.

The strain and strain-derived parameters, including global peak systolic strain values, peak systolic strain dispersion, and peak systolic strain relative dispersion, all did not differ significantly between all the three longitudinal views in each group, except that peak systolic strain relative dispersion showed a significant difference between the apical four chamber view and two chamber in CAV groups with no focal stenosis (table 12, figure 6).

Strain rate and strain-rate-derived parameters, including global peak longitudinal systolic strain rate, time to peak longitudinal systolic strain rate, and the ratio of global peak longitudinal systolic strain rate to time to peak longitudinal systolic strain rate, did not differ significantly between all three longitudinal views in patients with normal angiograms and CAV with no focal stenosis (table 18, figure 6). In CAV patients with focal stenosis, strain rate and strain rate-derived parameters showed a significant difference between apical four chamber views and apical long axial views, and between apical four and two chamber views.

Strain-derived synchrony parameters also did not differ different between all the three longitudinal views in each group, except that time to peak longitudinal systolic strain dispersion and one standard deviation of the time to peak longitudinal systolic strain dispersion were did differ significantly between the apical long axial views and apical two chamber views (table 21, figure 6).

These echocardiographic strain and strain rate imaging results may seem to reflect the fact that coronary allograft vasculopathy is a diffuse coronary artery disease, which affects the entire heart vessels.

The ROC analysis showed that time to peak systolic longitudinal strain rate and the ratio of global systolic longitudinal strain rate to time to peak systolic longitudinal strain rate in apical

four chamber view, apical long axial view, and apical two chamber view, respectively, had similar sensitivities and specificities with the same cut-off values in detecting CAV with no focal stenosis (table 26, 28, 30 and figure 7). The strain-derived synchrony parameters showed also similar sensitivities and specificities in the three longitudinal views with the same or similar cut-off values in detecting CAV with and without focal stenosis (table 33, and figure 8).

In our study, apical long axial view images were not available in three patients, and apical two chamber view images not in 40% patients, for strain and strain rate imaging, reflecting that the apical four chamber view is easier to record than the other apical views, especially the apical two chamber view.

These results suggest that the apical four chamber view may be substituted for the longitudinal three apical views in strain and strain rate imaging for prediction of CAV. TpSr in apical four chamber view of $\geq$ 129ms showed a positive predictive value of 88.4% and a negative predictive value of 80.7% for the prediction of CAV with no focal stenosis, and the combination of GSr and TpSr in apical four chamber view increased the positive and negative predictive values to 96.4% and 89.8%, respectively (table 34). The strain-derived synchrony parameters, including time to peak systolic strain dispersion, one standard deviation of the time to peak systolic strain, and intraventricular asynchrony index, in apical four chamber view showed high negative predictive values for the prediction of CAV with focal stenoses (86.7%, 89.2%, and 86.7%, respectively) (table 35).

Fourth, our results showed that STE-derived diastolic strain rate parameters may have limitations in the prediction of CAV.

In all the groups, the ratio of global diastolic early to late strain rate remained high ($GSr_E/GSr_A > 4$), reflecting the fact that diastolic function is abnormal early after heart transplantation and may persist following transplantation.[38] Conventional echocardiography showed a restrictive filling pattern after heart transplantation.

In the parasternal short axial view and apical longitudinal views, early and late global diastolic strain rate showed a significant reduction or a tendency towards a reduction in the CAV patients with no focal stenosis compared with the heart transplant recipients with normal angiograms and in the CAV patients without focal stenosis compared with the CAV patients with focal stenoses, but the discrepancy was too small to distinguish the patients with high predictive strength. The ratio of global diastolic early to late strain rate showed a tendency to an increase, with increased severity of angiographic lesions but no significant difference in all the groups. The time to peak

early diastolic strain rate showed also no significant difference in all the groups, except for time to peak radial early diastolic strain rate between the patients with and without focal stenosis.
In a study of PW-TDI[57], the diastolic PW-TDI parameters, including peak early diastolic wall motion velocity, early diastolic time and the ratio, showed no use for CAV diagnosis.

Last, it should be noted that the strain and strain rate values may be variable, depending on the technique used for strain imaging and tracking software.
By using the tracking software (Echo PAC 7.0, GE), we studied 56 patients with a mean of post-transplant duration of 1 year, who have normal coronary angiogram, and obtained the "normal" values for strain and strain rate in parasternal short axial and apical longitudinal views: global radial systolic strain (GSR) and strain rate (GSrR): 43.4±12.8% and 1.9±0.4 s^{-1}, global circumferential systolic strain (GSC) and stain rate (GSrC): 20.8±3.5 and -1.6±0.4 s^{-1}, global longitudinal systolic strain (GSL) and strain rate (GSrL) in four chamber, apical long axial, and two chamber views: -19.0±2.8%, -19.3±3.1%, 18.7±2.9% and -1.3±0.2 s^{-1}, -1.3±0.2 s^{-1}, -1.3±0.2 s^{-1}, respectively.
Our GSR value was very similar to the GSR values in the study by Marciniak et al[114] (43±11%). However, GSrR value in the study by Marciniak et al was very high in contrast to our GSrR value (4.0±1.0 s^{-1}). Marciniak et al recorded data from the posterior wall for radial strain and used strain by TDI.
Eroglu et al[124] reported "normal" post-Htx regional deformation values in 57 heart transplant recipients with a mean post-transplantation time of 5.5 years using a 2-D color Doppler-derived strain technique. Their GSL values in apical four and two chamber views were very similar to our values (-17±7.7%, -18.7±2.9%, respectively), but the GSrL values were a little higher than our values (-1.6±0.6 s^{-1}, -1.7±0.7 s^{-1}).
Saleh et al[128] reported the normal values for strain and systolic strain rate and synchrony of speckle-tracking echocardiography using velocity vector imaging (syngo VVI software) in 40 heart transplant recipients at 1 year after transplant. The GSL and GSrL values in apical four chamber, apical long axial, and apical two chamber views were relatively lower than our values (apical four chamber view: -13.62±3.21%, -0.82±0.25 s^{-1}, apical long axial view: -14.79±3.73%, -0.95±0.24 s^{-1}, apical two chamber view: -12.65±3.49%, 0.74±0.21 s^{-1}, respectively).
Syeda et al[129] studied 31 transplant patients with 10.6 years post-transplantation using speckle tracking software (Echo PAC 7.0,GE). They reported the GSL in apical four chamber, long axis, and two chamber views in patients without CAV, defined as multislice computed tomographic coronary angiography (MSCTA): -15±5.9%, -14±6.3%, and -14.3±7.3%, respectively. The

differences from our results may be attributed to the difference in the standard method for detecting of CAV. The main limitation of MSCT concerns the size of the vessels and the stenoses in small vessels, where CAV occurs early, and would be missed.[71]

The above study results may show the difference between myocardial strain images derived from velocity and speckle tracking and suggest that different speckle-tracking software for strain and strain rate imaging may result in different values of strain and strain rate.[87]

3.4.2. Pitfalls of STE diagnosis and study limitations

In contrast to TDI, speckle tracking is an angle independent technique as the movement of speckles in 2D gray-scale images can be followed in any direction.

However, speckle tracking echocardiography has a technical limitation of its dependence on frame rates. Low frame rate of gray-scale images may lead to undersampling, reducing peak Sr values, and rapid events in a cardiac cycle such as isovolumetric phases may not appear on images. Increasing the frame rate will result in a reduction of spatial resolution. Low frame rate increases the spatial resolution, but with too low a frame rate the speckle pattern could be outside of the search area, resulting in poor tracking. The optimal frame rate for speckle tracking appears to be 50-70 frames $_{/second}$.[87]

Changes in load conditions are important determinants of myocardial deformation. In our study, the possibility that reduction in strain and strain rate could be due to an increased wall stress cannot be entirely excluded. Left ventricular diastolic dimension increased, to a small extent, but significantly in the CAV patients without focal stenosis compared to the angiographically normal patients (4.8±0.4mm, and 4.6±0.5mm, respectively) and showed no significant difference between CAV patients with and without focal stenosis. Left ventricular diastolic wall thickness increased significantly in the CAV patients with focal stenosis compared to the patients with normal angiograms and CAV without focal stenosis. However, systolic aortic blood pressure did not differ significantly between the patients with normal angiogram and CAV with no focal stenoses, and between the CAV patients with and without focal stenoses. Diastolic blood pressure did not differ significantly between the three groups.

The necessity of high image quality limits the routine clinical applicability of the STE in all patients, especially after heart surgery. As mentioned above, in our study especially parasternal

short axis and apical two chamber views were not easily accessible to strain and strain rate imaging.

Data were obtained from a single-center retrospective study of prospectively gathered information.

Our data were also insufficient for serial long-term evaluations of strain and strain rate changes in the same patient after heart transplantation. Serial evaluation of strain and strain rate imaging in the same patients will probably yield more interesting data on the potential clinical usefulness of STE for post-transplant CAV surveillance.

3.5. Conclusion

Speckle tracking echocardiography appeared reliable for CAV prediction and for differentiation between patients with and without focal coronary stenoses.

The high predictive values of systolic strain dysynchrony and dyssynergy parameters recommend two dimensional strain as a noninvasive tool with the potential to facilitate early prediction of stenoses and to enable coronary angiographies to be timed, sparing patients frequent routine angiographies.

Summary

Bachgroud: The coronary allograft vasculopathy (CAV) is a major cause for the graft failure and one of leading causes for death after heart transplantation.

The routine annual coronary angiography is the standard for CAV surveillance. However, in many cases, coronary angiography may be insufficient for early CAV diagnosis before clinical events, and poses the risks.

The myocardial deformation analyses by strain imaging allow quantifying of change in myocardial function, that is not recognizable at visual assessment (e.g. longitudinal myocardial shortening), and distinction between active and passive wall motion.

We assessed the reliability of 2D speckle tracking derived strain imaging (STE) in distinguishing between patients with and without angiographic CAV for the optimal timing of coronary angiography.

Methods: left ventricular (LV) radial, circumferential and longitudinal strain and strain rate (Sr) were obtained in heart transplant recipients, with left ventricular ejection fraction (LVEF) of ≥55% and no visible regional wall motion abnormalities, by using speckle tracking software (EchoPAC 7.0). Dyssynchrony and dyssynergy indexes were calculated from strain and strain rate curves. Strain and Sr parameters and indexex were tested for relationships to angiographic findings. Angiographic evaluation of CAV was based on Stanford criteria. The patients with acute rejection, bundle branch block on ECG, and LVEF of <55% were excluded from the study.

Results: The coronary angiogram was normal in 56 patients (group 1). Angiograhic CAV was present in the other 146 patients, of which 87 patients had CAV with diffuse type B lesions but no focal stenosis (group 2), 59 patients with diffuse type B lesions and focal stenosis (group 3).

Whereas conventional echocardiographic parameters showed low sensitivities and specificities for CAV diagnosis, systolic STE parameters appeared highly predictive for detection of CAV. The time to peak longitudinal systolic strain rate of ≥129ms showed a positive predictive value of 88.4% and a negative value of 80.7% for the prediction of CAV with no focal stenosis. The global longitudinal acceleration of systolic deformation (ratio of global peak longitudinal systolic strain rate and time to peak longitudinal systolic strain rate) showed the highest positive and negative predictive values (96.4% and 89.8%, respetively) for the prediction of CAV with

no focal stenosis. The different dyssynchrony and dyssynergy parameters showed high negative predictive vales for the prediction of CAV with focal stenoses (86.7-89.2%).

Conclusions: our result showed that STE may be a reliable method for CAV surveillance. STE allowed differentiation between patients without CAV and patients with CAV, but normal LVEF and no visible regional wall motion abnormalities. The analyse of intraventricular synchrony and synergy enabled also early prediction of left ventricular dysfunction in CAV patients with focal stenoses, distinguishing between diffuse CAV with and without focal stenoses.

The high positive and negative predictive values of STE parameters may enable the optimal timing of coronary angiography for CAV surveillance.

References

1. Stehlik J, Edwards LB, Kucheryavaya AY, et al The Registry of the International Society for Heart and Lung Transplantation: Twenty-seventh official adult heart transplant report- 2010. J Heart Lung Transplant 2009;29(10):1089-103.

2. Uretsky BF, Murali S, Reddy S, et al Development of coronary artery disease in cardiac transplant patients receiving immunosuppressive therapy with cyclosporine and prednisone. Circulation 1987;76(4):827-34.

3. Aranda JM, Hill J. Cardiac Transplant Vasculopathy. CHEST 2000;118:1792-1800.

4. Uretsky BF, Kormos RL, Zerbe, et al Cardiac events after heart transplantation: incidence and predictive value of coronary arteriography. J Heart Lung Transplant 1992;11:S45-51.

5. Spes CH, Klauss V, Mudra H, et al Diagnostic and prognostic value of dobutamine stress echocardiography for noninvasive assessment of cardiac allograft vasculopathy :A comparison with coronary angiography and intravascular ultrasound. Circulation 1999;100:509-15.

6. Schmauss D, Weis M. Cardiac allograft vasculopathy, recent developments. Circulation 2008;117:2131-141.

7. Gao SZ, Alderman EL. Accelerated coronary vascular disease in the heart transplant patient: Coronary arteriographic findings. JACC 1988;12(2): 334-40.

8. Schroeder JS, Gao SZ, Hunt SA, et al Accelerated graft coronary artery disease: diagnosis and prevention. J Heart Lung Transplant 1992;11:S258-65.

9. Everett JP, Hershberger RE, Ratkovec RM, et al The specificity of normal qualitative angiography in excluding cardiac allograft vasculopathy. J Heart Lung Transplant 1994;13:142-8.

10. Brodaty D, Bonnet N, de Lentdecker P, et al A prospective comparative study of coronary angiography and endocoronary ultrasonography in the prediction of coronary lesions after transplantation. Arch Mal Coeur Vaiss 1998;91(2):225-30.

11. Claque JR, Cox ID, Murday AJ, et al Low clinical utility of routine angiographic surveillance in the prediction and management of cardiac allograft vasculopathy in transplant recipients. Clin Cardiol 2001;24(6):459-62.

12. Johnson DE, Alderman EL. Transplant coronary artery disease: histopathologic correlations with angiographic morphology. JACC 1991;17(2): 449-57.

13. St.Goar FG, Pinto FJ, Alderman EL, et al Intracoronary ultrasound in cardiac transplant recipients, In vivo evidence of " angiographically silent" intimal thickening. Circulation 1992;85:979-87.

14. Young JB, Smart FM, Lowry RL, et al Coronary angiography after heart transplant-ation: should study be the "gold standard"? J Heart Lung Transplant 1992;11:S65-8.

15. Mills RM, Hill JA, Theron HD, et al Serial quantitative coronary angiography in the assessment of coronary disease in the transplanted heart. J Heart Lung Transplant 1992;11:S52-5.

16. Keogh AM, Valantine HA, Hunt SA, et al Impact of proximal or midvessel discrete coronary artery stenoses on survival after heart transplantation. J Heart Lung Transplant 1992;11(5):892-901.

17. Bacal F, Moreira LF, Souza G, et al Dobutamine stress echocardiography predicts cardiac events or death in asymptomatic patients long-term after heart transplantation: 4-year prospective evaluation. J Heart Lung Transplant 2004;23:1238-44.

18. Young JB. Allograft vasculopathy: diagnosing the nemesis of heart transplantation. Circulation 1999;100:458-60.

19. Scheld HH, Deng MC, Hammel D. Langzeitkomplikationen/Nachsorge, Leitfaden Herztransplantation. Steinkopff Verlag, Darmstadt. 1997;173-86.

20. Pflugfelder PW, Boughner DR, Rudas L, et al Enhanced prediction of cardiac allograft disease with intracoronary ultrasonographic imaging. Am Heart J 1993;125:1583-91.

21. Kerber S, Rahmel A, Heinemann-Vechtel O, et al Angiographic, intravascular ultrasound and functional findings early after orthotopic heart transplantation. Int J Cardio 1995;49:119-29.

22. Tuzcu EM, Kapadia SR, Tutar E, et al High prevalence of coronary atherosclerosis in asymptomatic teenagers and young adults: evidence from intravascular ultrasound. Circulation 2001;103:2705-10.

23. Yeung AC, Davis SF, Hauptman PJ, et al Multicenter intravascular ultrasound transplant study group. Incidence and progression of transplant coronary artery disease over 1 year: results of a multicenter trial with use of intravascular ultrasound. J Heart Lung Transplant 1995;14:S215-20.

24. Kobashigawa JA, Tobis JM, Starling RC, et al Multicenter intravascular ultrasound validation study among heart transplant recipients. JACC 2005;45:1532-7.

25. Tuzcu EM, Kapadia SR, Sachar R, et al Intravasclar ultrasound evidence of angiographically silent progression in coronary atherosclerosis predicts long-term morbidity and mortality after cardiac transplantation. JACC 2005;45:1538-42.

26. Bocksch W, Wellnhofer E, Schartl M, et al Reproducibility of serial intravascular ultrasound measurements in patients with angiographically silent coronary artery disease after heart transplantation. Corn Artery Dis 2000;11(7):555-62.

27. Pinto FJ, St.Goar FG, Gao SZ, et al Immediate and one-year safety of intracoronary ultrasonic imaging. Evaluation with serial quantitative angiography. Circulation 1993;88:1709-14.

28. Hausmann D, Erbel R, Alibelli-Chemarin MJ, et al The safety of intracornary ultrasound. A multicenter survey of 2207 examinations. Circulation 1995;91:623-30.

29. Ramasubbu K, Schoenhagen P, Balghith MA, et al Repeated intravascular ultrasound imaging in cardiac transplant recipients dose not accelerate transplant coronary artery disease. JACC 2003;41:1739-43.

30. Mairesse GH, Marwick TH, Melin JA, et al Use of exercise electrocardiography, technetium-99m-MIBI perfusion tomography, and two-dimensional echocardiography for coronary disease surveillance in a low-prevalence population of heart transplant recipients. J Heart Lung Transplant 1995;14;229-9.

31. Smart FW, Ballantyne CM, Cocanougher B, et al Insensitivity of noninvasive tests to detect coronary artery vasculopathy after heart transplant. Am J Cardiol 1991;67: 243-7.

32. Ehrman JK, Keteyian SJ, Levine AB, et al Exercise stress tests after cardiac transplantation. Am J Cardiol 1993;71:1372-3.

33. Bacal F, Groppo Stolf NA, Veiga VC, et al Noninvasive diagnosis of allograft vascular disease after heart transplantation. Arq Bras Cardil 2001;76:36-42.

34. Kass M, Allan R, Haddad H. Diagnosis of graft coronary artery disease. Curr Opin Cardiol 2007;22:139-45.

35. Antunes ML, Spotnitz HM, Clark MB, et alLong- term function of human cardiac allografts assessed by two-dimensional echocardiography. J Thorac Cardiovasc Surg 1989;98:275-84.

36. Tischler MD, Lee RT, Plappert T, et al Serial assessment of left ventricular function and mass after orthotopic heart transplantation: a 4-year longitudinal study. JACC 1992;19:60-6.

37. Wilhelmi M, Pethig K, Nguyen H, et al Heart transplantation: echocardiographic assessment of morphology and function after more than 10 years of follow-up. Ann Thorac Surg 2002;74:1075-9.

38. St Goar FG, Gibbons R, Schnittger I, et al Left ventricular diastolic function: Doppler echocardiographic changes soon after cardiac transplantation. Circulation 1990;82:872-8.

39. Boissonnat P, Gare JP, de Lorgeril M, et al Evaluation of non invasive methods for the diagnosis of atherosclerosis of the graft after orthotopic cardiac transplantation. Arch Mal Coeur Vaiss 1992;85:1285-90.

40. Spes CH, Angermann CE. Stresss echocardiography for assessment of cardiac allograft vasculopathy. Z Kardiol 2000;89 Suppl 9: IX/50-3.

41. Collings CA, Pinto FJ, Valantine HA, et al Exercise echocardiography in heart transplant recipients: a comparison with angiography and intracoronary ultrasonography. J Heart Lung Transplant 1994;13:604-13.

42. Cohn JM, Wilensky RL, O'Donnell JA, et al Exercise echocardiography,angiography, and intracoronary ultrasound after cardiac transplantation. Am J Cardiol 1996;77:1216-9.

43. Ciliberto GR, Massa D, Mangiavacchi M, et al High-dose dipyridamole echocardiography test in coronary artery disease after heart transplantation. Eur Heart J 1993;14:48-52.

44. Akosah KO, Mohanty PK, Funai JT, et al Noninvasive prediction of transplant coronary artery disease by dobutamine stress echocardiography. J Heart Lung Transplant 1994;13:1024-38.

45. Günther F, Schwammenthal E, Rahmel A, et al Initial experiences with dobutamine stress echocardiography in heart transplant patients. Z Kardiol 1995;84:411-8.

46. Spes CH, Mudra H, Schnaack SD, et al Dobutamine stress echocardiography for noninvasive diagnosis of cardiac allograft vasculopathy: a comparison with angiography and intravascular ultrasoun. Am J Cardiol 1996;78:168-74.

47. Derumeaux G, Redonnet M, Mouton-Schleifer D, et al Dobutamine stress echocardiography in orthotopic heart transplant recipients. JACC 1995;25:1665-72.

48. Spes CH, Mudra H, Schnaack SD, et al Quantitative dobutamine stress echocardiography in follow-up of heart transplantation: normal values and findings in patients with transplant vasculopathy. Z Kardio 1997;86:868-76.

49. Akosah KO, McDANIEL S, Hanrahan J, et al Dobutamine stress echocardiography early after heart transplantation predictis development of allograft coronary artery disease and outcome. JACC 1998;31:1607-14.

50. Spes CH, Klauss V, Mudra H, et al Diagnostic and prognostic value of serial dobutamine stress echocardiography for noninvasive assessment of cardiac allograft vasculopathy: A comparison with coronary angiography and intravascular ultrasound. Circulation 1999;100:509-15.

51. Otto CM, Marwick TH. Stress echocardiography with nonexercise techniques, The practice of clinical echocardiography 3th. Saunders Elsevier 2007;353-84.

52. Rodrigues A.C.T., Bacal F, Medeiros CC, et al Noninvasive prediction of coronary allograft vasculopathy by myocardial contrast echocardiography. J Am Echocardiogr 2005;18:116-21.

53. Tona F, Caforio A.L.P., Montisci R, et al Coronary flow velocity pattern and coronary flow reserve by contrast-enhanced transthoracic echocardiography predict long-term outcome in heart transplantation. Circulation 2006;114(suppl I):I49-55.

54. Hacker M, Hoyer HX, Uebleis C, et al Quantitative assessment of cardiac allograft vasculopathy by real-time myocardial contrast echocardiography: a comparison with conventional echocardiographic analyses and Tc99m-sestamibi SPECT: Eur J Echocardiogr 2008;9:494-500.

55. Tona F, Caforio A.L.P., Montisci R, et al Coronary flow reserve by contrast-enhanced echocardiography: A new noninvasive diagnostic tool for cardiac allograft vasculopathy. Am J Transplant 2006;6;998-1003.

56. Tona F, Osto E, Tarantini G, et al Coronary flow reserve by transthoracic echocardiography predicts epicardial intimal thickening in cardiac allograft vasculopathy. Am J Transplant 2010;10;1677-85.

57. Dandel M, Hummel M, Müller J, et al Reliability of tissue doppler wall motion monitoring after heart transplantation for replacement of invasive routine screenings by optimally timed cardiac biopsies and catheterizations. Circulation 2001;104(suppl I):I184-191.

58. Knollmann FD, Bocksch W, Spiegelsberger S, et al Electron-beam computed tomography in the assessment of coronary artery disease after heart transplantation. Circulation 2000;101:2078-82.

59. Dandel M, Knollmann F, Wellnhofer E, et al Noninvasive strategy for early prediction of transplant coronary arteriopathy and timing of coronary angiographies in heart transplant recipients. Frontiers in coronary artery disease, Proceedings of the 5th international congress on coronary artery disease Florence,Italy,October 19-22,2003.

60. Giliberto GR, Mangiavacchi M, Banfi F, et al Coronary artery disease after heart transplantation: non-invasive evaluation with exercise thallium scintigraphy. Eur Heart J 1993;14:226-9.

61. Rodney RA, Johnson LL, Blood DK, et al Myocardial perfusion scintigraphy in heart transplant recipients with and without allograft atherosclerosis: a comparison of thallium-201 and technetium 99m sestamibi. J Heart Lung Transplant 1994;13:173-80.

62. Howarth M, Forstrom A, Samudrala V, et al Evaluation of ^{201}Tl SPECT myocardial perfusion imaging in the prediction of coronary artery disease after orthotopic heart tranplantation. Nucl Med Commun 1996;17:105-13.

63. Redonnet M, Derumeaux G, Mouton-Schleifer D, et al Noninvasive prediction of cardiac graft vascular disease. Transplant Proc 1995;27:2530-1.

64. Carlsen J, Toft JC, Mortensen SA, et al Myocardial perfusion scintigraphy as a screening method for significant coronary artery stenosis in cardiac transplant recipients. J Heart Lung Transplant 2000;19:873-78.

65. Wu YW, Yen RF, Lee CM, et al Diagnostic and prognostic value of dobutamine thallium-201 single-photon emission computed tomography after heart transplantation. J Heart Lung Transplant 2005;24:544-50.

66. Elhendy A, van Domburg RT, Vantrimpont P, et al Prediction of mortality in heart transplant recipients by stress technetium-99m tetrofosmin myocardial perfusion imaging. Am J Cardiol 2002;89:964-8.

67. McKillop JH, Goris ML. Thallium-201 myocardial imaging in patients with previous cardiac transplantation. Clinical Radiology 1981;32:447-9.

68. Puskas C, Kosch M, Kerber S, et al Progressive heterogeneity of myocardial perfusion in heart transplant recipients detected by thallium-201 myocardial SPECT. J Nucl Med 1997;38:760-5.

69. Legare JF, Haddad H, Bames D, et al Myocardial scintigraphy correlates poorly with coronary angiography in the screening of transplant arteriosclerosis. Can J Cardio 2001;17:866-72.

70. Kerber S, Puschkas C, Jonas M, et al Can Tl-201 myocardial SPECT abnormalities in orthotopic heart recipients be explained by coronary vessel wall alterations assessed by intravascular ultrasoun? Int J Cardiol 1996;57:91-6.

71. Romeo G, Houyel L, Angel CY, et al Coronary stenosis prediction by 16-slice computed tomography in heart transplant patients: Comparison with conventional angiography and impact on clinical management. JACC 2005;45:1826-31.

72. Sigurdsson G, Carrascosa P, Yamani MH, et al Prediction of transplant coronary artery disease using multidetector comptude tomography with adaptative multisegment reconstruction. JACC 2006;48:772-8.

73. Nunoda S, Machida H, Sekikawa A, et al Evaluation of cardiac allograft vasculopathy by multidetector computed tomography and whole-heart magnetic resonance coronary angiography. Circ J 2010;74:946-53.

74. Iyengar S, Feldman D, Cooke GE, et al Prediction of coronary artery disease in orthotopic heart transplant recipients with 64-Detector row computed tomography angiography. J Heart Lung Transplant 2006;25:1363-6.

75. Barbir M, Lazem F, Bowker T, et al Determinants of transplant-related coronary calcium detected by ultrafast computed tomography scanning. Am J Cardiol 1997;79:1606-09.

76. Shemesh J, Tenenbaum A, Stroh CI, et al Double-helical CT as a new tool for tracking of allograft atherosclerosis in heart transplant recipients. Invest Radio 1999;34:485-8.

77. Ludman PF, Lazem F, Barbir M, et al Incidence and clinical relevance of coronary calcification detected by electron beam computed tomography in heart transplant recipients. Eur Heart J 1999;20:303-8.

78. Ratliff NB III, Jorensen CR, Gobel FL, et al Lack of usefulness of electronbeam computed tomography for detecting coronary allograft vasculopathy. Am J Cardiol 2004;94:202-6.

79. Caus T, Kober F, Marin P, et al Non-invasive diagnostic of cardiac allograft vasculopathy by 31 P magnetic resonance chemical shift imaging. Eur J Cardiothorac Surg 2006;29:45-9.

80. Muehling OM, Wilke NM, Panse P, et al Reduced myocardial perfusion reserve and tranmural perfusion gradient in heart transplant arteriopathy assessed by magnetic resonance imaging. JACC 2003;42:1054-60.

81. Korosoglou G, Osman NF, Dengler TJ, et al Strain-encoded cardiac magnetic resonance for the evaluation of chronic allograft vasculopathy in transplant recipients. Am J Transplant 2009;9:2587-96.

82. Zhao XM, Delbeke D, Sandler MP, et al Nitrogen-13-ammonia and PET to detect allograft coronary artery disease after heart transplantation: Comparison with coronary angiography. J Nucl Med 1995;36:982-7.

83. Allen-Auerbach M, Schröder H, Johnson J, et al Relationship between coronary function by positron emission tomography and temporal changes in morphology by intravascular ultrasound (IVUS) in transplant recipients. J Heart Lung Transplant 1999;18:211-19.

84. Wolpers HG, Köster C, Burchert W, et al Coronary reserve after orthotopic heart transplantation: quantification with N-13 ammonia and positron emission tomography. Z Kardiol 1995;84:112-20.

85. Wu YW, Chen YH, Wang SS, et al PET assessment of myocardial perfusion reserve inversely correlates with intravascular ultrasound findings in angiographically normal cardiac transplant recipients. J Nucl Med 2010;51:906-12.

86. Otto CM, Smiseth OA, Edvardsen T. Tissue doppler and speckle tracking echocardiography, The practice of clinical echocardiography 3th. Saunders Elsevier 2007;115-33.

87. Dandel M, Lehmkuhl H, Knosalla C, et al Strain and strain rate imaging by echocardiography – Basic concepts and clinical applicability. Curr Cardiol Review 2009;5:133-48.

88. Mirsky I, Pasternac A, Ellison RC. General index for the assessment of cardiac function. Am J Cardiol 1972;30:483-91.

89. Mirsky I, Parmley WW. Assessment of passive elastic stiffness for isolated heart muscle and the intact heart. Circ Res 1973;33:233-43.

90. D'hooge J, Heimdal A, Jamal F, et al Regional strain and strain rate measurements by cardiac ultrasound: principles, implementation nad limitations. Eur J Echocardiography 2000;1:154-170.

91. Stoylen A, Heimdal A, Bjornstad K, et al Strain rate imaging by ultrasound in the diagnosis of regional dysfuction of the left ventricle. Echocardiography 1999;16:321-29.

92. Urheim S, Edvardsen T, Torp H, et al Myocardial strain by doppler echocardiography, validation of a new method to quantify regional myocardial function. Circulation 2000;102:1158-64.

93. Perk G, Tunick PA, Kronzon I. Non-doppler two-dimensional strain imaging by echocardiography – from technical considerations to clinical applications. J Am Soc Echocardiogra 2007;20:234-43.

94. Marwick TH. Measurement of strain and strain rate by echocardiography, ready for prime time? JACC 2006;47:1313-27.

95. Jamal F, Sutherland GR, Weidemann F, et al Can changes in systolic longitudinal deformation quantify regional myocardial function after an acute infarction? An ultrasonic strain rate and strain study. J Am Soc Echocardiogr 2002;15:723-30.

96. Williams RI, Payne N, Phillips T, et al Strain rate imaging after dynamic stress provides objective evidence of persistent regional myocardial dysfuction in ischemic myocardium: regional stunning identified? Heart 2005;91:152-60.

97. Liang HY, Cauduro S, Pellikka P, et al Usefulness of two-dimensional speckle strain for evaluation of left ventricular diastolic deformation in patients with coronary artery disease. Am J Cardiol 2006;98:1581-6.

98. Nucifora G, Schuijf JD, Delgado V, et al Incremental value of subclinical left ventricular systolic dysfunction for the identification of patients with obstructive coronary artery disease. Am Heart J 2010;159:148-57.

99. Yip G, Khandheria B, Belohlavek M, et al Strain echocardiography tracks dobutamine-induced decrease in regional myocardial perfusion in nonocclusive coronary stenosis. JACC 2004;44:1664-71.

100. Voigt JU EB, Schmiedehausen K, Huchzermeyer C, et al Strain-rate imaging during dobutamine stress echocardiography provides objective evidence of inducible ischemia. Circulation 2003;107:2120-6.

101. Hanekom L, Cho GY, Leano R, et al Comparison of two dimensional speckle and tissue doppler strain measurement during dobutamine stress echocardiography: an angiographic correlation. Eur Heart J 2007;28:1765-72.

102. Ng AC, Sitges M, Pham PN, et al Incremental value of 2-dimensional speckle tracking strain imaging to wall motion analysis for prediction of coronary artery disease in patients undergoing dobutamine stress echocardiography. Am Heart J 2009;158:836-44.

103. Ishii K, Imai M, Suyama T, et al Exercised-induced post-ischemic left ventricular delayed relaxation or diastolic stunning: is it a reliable marker in prediction coronary artery disease? JACC 2009;53:698-705.

104. Jurcut R, Pappas CJ, Masci PG, et al Prediction of regional myocardial dysfunction in patients with acute myocardial infarction using velocity vector imaging. J Am Soc Echocardiogr 2008;21:879-86.

105. Gjesdal O, Hopp E, Vardal T, et al Global longitudinal strain measured by two-dimensional speckle tracking echocardiography is closely related to myocardial infarct size in chornic ischaemic heart disease. Clin Sci (Lond) 2007;113:287-96.

106. Delgado V, Mollema SA, Ypenburg C, et al Relation between global left ventricular longitudinal strain assessed with novel automated function imaging and biplane left ventricular ejection fraction in patients with coronary artery disease. J Am Soc Echocardiogr 2008;21:1244-50.

107. Park YH, Kang SJ, Song JK, et al Prognostic value of longitudinal strain after primary reperfusion therapy in patients with anterior-wall acute myocardial infarction. J Am Soc Echocardiogr 2008;21:262-7.

108. Jamal F, Strotmann J, Weidemann F, et al Noninvasive quantification of the contractile reserve of stunned myocardium by ultrasonic strain rate and strain. Circulation 2001;104:1059-65.

109. Migrino RQ, Zhu X, Pajewski N, et al Assessing of segmental myocardial viability using regional 2-dimensional strain echocardiography. J Am Soc Echocardiogr 2007;20:342-51.

110. Mollema SA, Delgado V, Bertini M, et al Viability assessment with global left ventricular longitudinal strain predicts recovery of left ventricular function after acute myocardial infarction. Circ Cardiovasc Imaging 2010;3:15-23.

111. Marciniak A, Claus P, Sutherland GR, et al Changes in systolic left ventricular function in isolated mitral regurgitation. A strain rate imaging study. Eur Heart J 2007;28:2627-36.

112. Kepez A, Akdogan A, Sade LE, et al Prediction of subclinical cardiac involvement in systemic sclerosis by echocardiographic strain imaging. Echocardiography 2008;25:191-7.

113. Hare JL, Brown JK, Marwick TH. Association of myocardial strain with left ventricular geometry and prognosis of hypertensive heart disease. Am J Cardiol 2008;102:87-91.

114. Marciniak A, Sutherland GR, Marciniak M, et al Myocardial deformation abnormalities in patients with aortic regurgitation: a strain rate imaging study. Eur J Echocardiogr 2009;10:112-9.

115. D' Andrea A, Stisi S, Gao P, et al Associations between left ventricular myocardial involvement and endothelial dysfunction in systemic sclerosis: noninvasive assessment in asymptomatic patients. Echocardiography 2007;24:587-97.

116. Galderisi M, de Simone G, Inneli P, et al Impaired inotropic response to type 2 diabetes mellitus: a strain rate imaging study. Am J Hypertens 2007;20:548-55.

117. Bellavia D, Abraham TP, Pellikka PA, et al Prediction of left ventricular systolic dysfunction in cardiac amyloidosis with strain rate echocardiography. J Am Soc Echocardiogr 2007;20:1194-202.

118. Yu CM, Zhang Q, Fung JW, et al: A novel tool to assess systolic asynchrony and identify responders of cardiac resynchronization therapy by tissue synchronization imaging. JACC 2005;45:677-84.

119. Gorcsan III J, Kanzaki H, Bazaz R, et al Usefulness of echocardiographic tissue synchronization imaging to predict acute response to cardiac resynchronization therapy. Am J Cardiol 2004;93:1178-81.

120. Suffoletto MS, Dohi K, Cannesson M, et al Novel speckle-tracking radial strain from routine black-white echocardiographic images to quantify dysynchrony and predict response to cardiac resynchronization therapy. Circulation 2006;113:960-8.

121. Dandel M, Suramelasvili N, Lehmkuhl H, et al 2D strain echocardiography a novel non-invasive tool for pretransplant evaluation of patients with dilated cardiomyopathy. J Heart Lung Transplant 2007;26:S239.

122. Jasaityte R, Dandel M, Lehmkuhl H, et al Prediction of short-term outcomes in patients with idiopathic dilated cardiomyopathy referred for transplantation using standard echocardiography and strain imaging. Transplant Proc 2009;41:277-80.

123. Pieper GM, Shah A, Harmann L, et al Speckle-tracking 2-dimensional strain echocardiography: a new noninvasive imaging tool to evaluate acute rejection in cardiac transplantation. J Heart Lung Transplant 2010;29:1039-46.

124. Eroglu E, Herbots L, Cleemput JV, et al Ultrasonic strain/strain rate imaging- a new clinical tool to evaluate the transplanted heart. Eur J Echocardiogr 2005;6:186-95.

125. Marciniak A, Eroglu E, Marciniak M, et al The potential clinical role of ultrasonic strain and strain rate imaging in diagnosing acute rejection after heart transplantation. Eur J Echocardiogr 2007;8:213-21.

126. Kato TS, Oda N, Hashimura K, et al Strain rate imaging would predict sub-clinical acute rejection in heart transplant recipients. Eur J Cardio-thoracic Sur 2010;37:1104-10.

127. Dandel M, Wellnhofer E, Lehmkuhl H, et al Early detection of left ventricular wall motion alterations in heart allografts with coronary artery disease: diagnostic value of tissue Doppler and two-dimensional (2D) strain echocardiography. Eur J Echocardiogr 2006;7:S127-8

128. Saleh HK, Villarraga HR, Kane GC, et al Normal left ventricular mechanical function and synchrony values by speckle-tracking echocardiography in the transplanted heart with normal ejection fraction. J Heart Lung Transplant 2011;30:652-8.

129. Syeda B, Höfer P, Pichler P, et al Two-dimensional speckle-tracking strain echocardiography in long-term heart transplant patients: a study comparing deformation parameters and ejection fraction derived form echocardiography and multislice computed tomography. Eur J Echocardiogr 2011;12:490-6.

130. Eroglu E, D'hooge J, Sutherland GR, et al Quantitative dobutamine stress echocardiography for the early prediction of cardiac allograft vasculopathy in heart transplant recipients. Heart 2008;94:e1-7.

Anhang

Danksagen

Bedanken möchte ich mich bei Herrn Prof. Dr. med. Dr. hc. mult. R. Hetzer, ärztlichem Direktor des Deutschen Herzzentrums Berlin, für die Einladung zur medizinischen Fortbildung und für die Unterstützung meiner Tätigkeit im Deutschen Herzzentrum Berlin.

Meinen besonderen Dank für die Betreuung und Unterstützung möchte ich an meinen Doktorvater, Herrn Priv. - Doz. Dr. med. M. Dandel, der auf mich unvergessliche und tiefe Eindrücke gemacht hat.

Ganz besonders danken möchte ich meiner Frau, Un Hui, Jong, die mich stets bestärkt und unterstützt hat und daher widme ich ihr diese Arbeit.

Lebenslauf

Mein Lebenslauf wird aus datenschutzrechtlichen Gründen in der elektronischen Version meiner Arbeit nicht veröffentlicht.

Liste der Publikationen

1. Pang CH, Dandel M, Wellnhofer E, et al Usefulness of echocardiographic myocardial deformation analysis by strain imaging for detection of patients with coronary stenoses after heart transplantation (abstract).
   The Heart Surgery Forum 2011;14:S39-40.

   Diser Artikel wurde als Vortrag auf dem WSCTS 2011 in Berlin (World Society of Cardio-Thoracic Surgeon: 21st World Congress 12.-15. Juni 2011) präsentiert.

2. Pang CH, Dandel M, Wellnhofer E, et al Myocardial deformation analysis by echocardiographic strain imaging allows differentiation between patients with and without coronary stenoses after heart transplantation (abstract).
   Transplant International 2011;24 (Suppl.3),5.

   Diser Artikel wurde als Vortrag für die 20. Jahrestagung der Deutschen Transplantationsgesellschaft in Regensburg (6.-8. Oktober 2011) präsentiert.

3. Dandel M, Pang CH, Wellnhofer E, et al Echocardiographic strain imaging allows differentiation between heart transplant recipients with and without coronary stenoses (abstract). Circulation 2011;124:A9 162.

Erklärung

Ich, Chol Ho, Pang, erkläre, dass ich die vorgelegte Dissertation mit dem Thema:

Reliability of echocardiographic myocardial deformation analysis by speckle tracking for detection of patients with cardiac allograft vasculopathy after heart transplantation

selbst verfasst und keine anderen als angegebenen Quellen und Hilfsmittel benutze, ohne die (unzulässige) Hilfe Dritter verfasst und auch in Teilen keine Kopien anderer Arbeiten dargestellt habe.

Datum Unterschrift